

APPENDIX A

NUMERICAL MODELLING AUDITS

A.1 PART 1 OF THE SOFT AUDIT: 'ROBUSTNESS QUESTIONS'

1. What is the purpose of the modelling?

To investigate the mechanics of valley closure and upsidence using the block movement theory.

2. In what way is this work different to previous similar modelling work?

To the best of the author's knowledge, modelling valley closure and upsidence using block movements has never been attempted before.

3. What is the scale of the rock mass being modelled?

Large scale models with dimensions measured in the order of several hundred metres.

4. What is the basic modelling geometry?

For the isolated single panel models, the geometry encompasses everything from below the longwall up to the surface. For the river valley models, only the first few rock strata was modelled, with the replication of the subsidence profile being achieved by 'pulling down' the base of the models. The width of all models was defined by the distance at which a full subsidence profile could be developed.

- 5. Has it been necessary to divide the rock mass into separate rock mass domains? (Rock mass domain: a region of the rock mass in which the rock properties are statistically similar, but different to the properties of the surrounding rock in other structural domains)**

Yes, in the isolated single panel models there were 19 separate rock mass domains representing the different strata units. In the river valley models there were four separate rock mass domains.

- 6. Are the intact rock properties being specifically incorporated?**

Yes.

- 7. How are the fracture properties being incorporated?**

The fracture properties are incorporated by way of the numerical modelling code's nature. The numerical code used (UDEC) is a Distinct Element code. Tools like ubiquitous joints were not used at all.

- 8. Are features of the structural geology of the rock mass being incorporated?**

Yes. Bedding plane spacing, sub-vertical joint spacing and sub-vertical joint dip are incorporated. The strata units were assumed to be perfectly horizontal.

- 9. Are the rock mass properties being input directly (as opposed to being a result of the input intact rock and fracture properties)?**

No. The intact properties for the blocks together with the presence of joints in the model were assumed to produce realistic rock mass strength.

- 10. How have the rock mass properties been estimated?**

The majority of the intact rock properties were estimated by laboratory triaxial testing. The material properties that were missing were obtained from the literature,

and if partial material properties were available the remainder were estimated using the Mohr-Coulomb failure criterion. The presence of joints was expected to result in a realistic rock mass strength.

11. Is a constitutive law required for the rock mass? If so, how was it established?

The rock mass was assumed to conform to the Mohr-Coulomb constitutive law given that some material properties were estimated using this constitutive law.

12. Has the rock mass been modelled as a CHILE material? (CHILE: Continuous, homogenous, isotropic, linearly elastic.) What has been done to account for the DIANE aspects of the rock reality (DIANE: Discontinuous, inhomogeneous, anisotropic, not elastic)

DIANE. The numerical code automatically accounts for the DIANE aspects of the rock reality.

13. How have the stress boundary conditions been established?

Stress boundary conditions were not used. An in-situ stress regime with fixed boundaries was utilised instead.

14. Does the model include any failure criteria. If so, which one(s)?

The rock mass is governed by the Mohr-Coulomb plasticity failure criterion. The joints are governed by the Joint Area Contact model which is a Coulomb slip model with residual strength.

15. Is the rock being modelled as a continuum, discontinuum, or combination of the two?

Discontinuum.

16. What are the hydrogeological conditions in the model?

Hydrogeological conditions were not incorporated.

17. How have the hydrological boundary conditions been established?

Hydrogeological boundary conditions were not incorporated.

18. Are effective stresses being used?

No.

19. How are the thermal properties being incorporated?

Thermal properties were not incorporated.

20. How are the THM components being included in the modelling: as uncoupled components, pairwise coupled components, fully coupled components?

Only the mechanical components are being modelled.

21. Are there any special boundary conditions, loading conditions, or rock mass features in the modelling?

There are no special boundary conditions or rock mass features in the modelling.
The loading conditions consist of the establishment of an in-situ stress regime.

22. Has physical rock testing been used to obtain any parameters in the modelling?

Yes.

23. Has there been any study of potential adverse interactions that could lead to positive feedbacks and hence instabilities – in the rock mass and in the modelling?

Yes. In the isolated single panel models there was some concern that the instantaneous extraction of the longwall could shock the model. Different damping mechanisms for these models were tried, including a quasi-elastic sub stage, but the final results were very similar. In the river valley models, it was necessary to experiment and find what the most suitable velocity displacement profile could be applied to the base of the models to avoid premature rock mass failure but still maximise developed subsidence.

24. Have all the potential failure mechanisms been identified?

Yes. Cave zones, bedding plane dilation, vertical cracks and spanning rock beams have been identified in the literature and observed in the numerical models.

25. Have modelling sensitivity studies been undertaken?

Yes. Basic sensitivity analysis on mesh density, joint friction angle and joint cohesion has been performed on the river valley models.

26. Have modelling protocols been used?

Yes.

27. How will the modelling methods and results be presented?

The modelling results are presented as a series of tables and graphs.

28. Can the modelling be verified/validated? – in this study and in principle?

Yes, the modelling has been verified by empirical techniques. The analytical techniques produced good matches but cannot be used as verification tools as they are designed to work on much simpler systems.

29. Are there any features of the model or modelling work not covered by the points above?

No.

**A.2 PART 2 OF THE SOFT AUDIT: SPECIFYING THE COMPONENTS
AND FEATURES OF THE MODELLING**

1. THE MODELLING OBJECTIVE

1.1. Has the modelling objective been clearly established?

Yes, the modelling objective has been clearly established. The main objective was to investigate if the proposed block movement model is feasible for the tilts and curvatures generated in the Southern Coalfield. For this to occur, the models must conform to observed subsidence behaviour in the Southern Coalfield.

1.2. How will it be known when the modelling work is completed?

The modelling work, in keeping with the objectives of this thesis, is complete.

2. CONCEPTUALISATION OF THE PROCESSES BEING MODELLED

2.1. What rock mass systems are being considered?

The rock mass includes 19 different rock types.

2.2. What are the main physical processes being modelled?

The main physical processes being modelled in the isolated single panel models are the extraction of the longwall, the subsequent formation of the cave zone and the resulting deformation on the ground surface. The main physical processes being modelled in the river valley models are the replication of the surface subsidence profile by ‘pulling down’ the base of the model and the resulting valley closure and upsidence.

3. SPECIFICATION OF THE MODELLING CONTENT

3.1. Is the model 1D, 2D, 3D or some combination?

The model is 2D.

3.2. Is a continuum or a discontinuum being modelled?

A discontinuum is being modelled.

3.3. Specification of the boundary conditions.

The isolated single panel models have their boundaries fixed in the x and y-directions at the sides and base of the models. The top of the models is a free surface. The river valley models have their sides fixed in the x and y directions whilst the base is only fixed in the x direction. A velocity displacement profile is applied at the base of the models to replicate the surface subsidence profile. The top of the models is a free surface.

3.4. Specification of the initial conditions.

The initial conditions consist of implementing gravity and an in-situ stress regime. This is done for both the isolated single panel models and the river valley models. The models are then cycled to equilibrium to obtain the initial conditions.

3.5. How is the final condition established?

For the isolated single panel models, the final condition is established after the longwall is excavated and the model is allowed to cycle until the subsidence reaches a maximum value and remains constant. For the river valley models, the final condition is established when maximum developed subsidence on the surface reaches a prescribed value, and the models are cycled for an additional period of time to ensure final equilibrium.

4. MODELLING SOLUTION REQUIREMENTS

4.1. What is the required model output?

For the isolated single panel models, the required model output includes the x and y movement on the surface, the deflection of the Bulgo Sandstone and the visual indication of a goaf angle. For the river valley models, the required model output includes the x-displacements of the valley shoulders, the x-displacements of the valley base, y-displacements of the valley centres, horizontal stresses beneath the sides of the valley, and a visual indication of valley base yield, translation plane slip and buckling.

4.2. Does the model output match the modelling objectives?

Yes. The outputs listed for the isolated single panel models are used to calculate maximum developed subsidence, goaf edge subsidence, strains, tilt, inflection point location and goaf angle. These parameters are necessary for verification with empirical and analytical techniques. The outputs listed for the river valley models are used to determine whether rock blocks are rotating, calculate valley closure and upsidence, and valley base yield. These parameters are necessary for verification with analytical techniques.

5. MODELLING SOLUTION TECHNIQUE

5.1. In principle, how is the model output to be obtained: one code, one set of data, one run? – or a suite of numerical experiments?

The model output is obtained by a suite of numerical experiments. The isolated single panel models were designed to cover a portion of mining geometries in the Southern Coalfield and the river valley models were designed to test river valley response in relation to its transverse distance from a longwall and its vertical distance from a translation plane.

5.2. Are any quality control checks in place? Checking the input data have been entered correctly, validation against known solutions, independent duplication of runs?

Yes. Each script was carefully checked numerous times for errors as the models were run in a batch and any errors would not have been detected until the models had finished running, in some cases this took two weeks. The isolated single panel models and river valley models were verified with empirical and analytical data.

6. NUMERICAL CODE UTILISED

6.1. Which numerical code is to be used?

UDEC – Universal Distinct Element Code.

6.2. Why is that code being used?

UDEC is being used because of its ability to model discontinuous rock masses. This is paramount as the rock masses being modelled are blocky with well defined discontinuities.

6.3. Where did the code originate from?

The code has its origins in Cundall (1971) and is intended for analysis of rock engineering projects where potential modes of failure are directly related to the presence of discontinuous features.

6.4. How has the code been validated?

The code has been validated by the numerous simulations that are performed and verified by analytical techniques. These simulations are available in the UDEC User's Guide (Itasca 2000).

7. SUPPORTING MODEL DATA AND DATA INPUT METHOD

7.1. Listing of type and justification of boundary conditions.

For all models, the surface did not contain any boundary conditions as it represented the ground surface which is naturally free of conditions. In all models, the left hand and right hand sides of the models were fixed in the x and y-directions. This decision was made after it was found that the in-situ stresses at the side boundaries were not affected by the longwall excavation. In the isolated single panel models, the base was fixed in the y-direction so the entire model would not move downwards en masse. In the river valley models, the base was subjected to a displacement boundary in order to replicate the subsidence profile observed in the isolated single panel models. This was also done to drastically reduce the modelling time required.

7.2. Listing of input data with source of the data and justification.

Model geometries

- Holla and Barclay (2000).

Material properties

- CSIRO Petroleum (2002),
- MacGregor and Conquest (2005),
- McNally (1996),
- Pells (1993), and
- Williams and Gray (1980).

Bedding plane/sub-vertical joint spacing, properties and assumptions

- Author's field visits,
- Badelow et al. (2005),
- Barton (1976),
- Chan, Kotze and Stone (2005),
- Coulthard (1995),
- Ghobadi (1994),
- Itasca (2000),
- Mandl (2005),
- Pells (1993),
- Price (1966),
- Selley (2003), and
- Tucker (2003).

In-situ stress

- CSIRO Petroleum (2002).

Mesh generation

- Coulthard (1995).

It can be seen that all the input data is fully traceable and comes from reputable sources. Any assumptions are clearly stated.

7.3. Do the data have to be adjusted before being input?

No. Transparency and traceability were the main objectives of the input data.

8. MODEL SENSITIVITY ANALYSIS

8.1. How does the model output depend on the input parameter values?

The model is very geometrically dependent as there is a wide variation in results for the isolated single panel models. Although not tested, it is expected that differences in material/joint properties and spacings would also have a significant effect on the model output. In the river valley models, an increase in the translation plane joint cohesion and friction angle reduced the magnitude of valley closure.

8.2. Is a sensitivity analysis being conducted? If so, what type of analysis?

Processes, mechanisms, parameters, boundary conditions, couplings etc.

Yes, a basic sensitivity analysis was performed on the river valley models by varying the joint friction angle and joint cohesion of the translation plane.

8.3. How are the results of the sensitivity analysis to be summarised?

Table format and graphs.

9. PRESENTATION OF MODELLING RESULTS

9.1. Is it possible to demonstrate that the numerical code is operating correctly?

Yes. The verification carried out is evidence of this.

9.2. Is it possible to show that the supporting data are reasonable assumptions for a rock mass?

Yes, the verification also proves this point, as does the sources cited.

9.3. How are the modelling results to be presented?

The modelling results are presented as figures, tables and graphs. For the verification purposes, the modelling results are overlain onto empirical graphs.

9.4. Does the presentation of the modelling results link with the modelling objective?

Yes. Ultimately it was able to be shown by graphs, tables and visual representations of the models that valley closure and upsidence was caused by block movements.

10. SOURCES OF ERRORS

10.1. Have you already corrected any errors?

Yes. Any errors evident at the time of model execution have been corrected.

10.2. List the sources of potentially significant errors.

- Typographical mistakes,
- Incorrect material and joint properties,
- Incorrect in-situ stress regime, and
- Boundaries too close to excavation.

10.3. Do any of the potentially significant errors invalidate the modelling objective, concept and conclusions?

Yes they would because it could mean that the subsidence parameters are not being correctly simulated, simulated sub-surface deformations are not in accordance with the literature and observed behaviour, which has implications for individual block movements and hence the concept of the block movement model.

11. MODELLING ADEQUACY

11.1. Do all the previous questions indicate that in principle the model is adequate for the purpose?

Yes.

11.2. If not, list the problem areas

Not applicable.

11.3. What corrective action is required?

Not applicable.

11.4. Does the soft audit have to be repeated after corrective action has been taken?

No.

A.3 DEVELOPING FROM THE SOFT AUDIT TO THE HARD AUDIT

The process of developing a soft audit to a hard audit involves the same subjects and questions as the soft audit but including detailed justifications to the questions. The procedure for developing a soft audit to hard audit can be seen in Figure A.1.

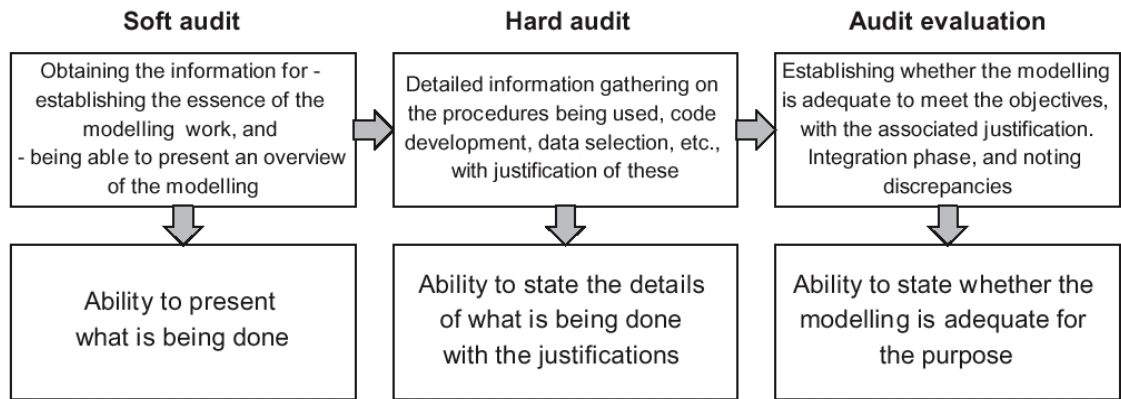


**Fig. A.1 – The procedure for developing from the soft audit to the hard audit
(Hudson, Stephansson & Andersson 2005)**

It can be seen in Section A.2 that the justifications have been included to the answers of the soft audit and the final answer is that the modelling is adequate for the purposes stated.

APPENDIX B

SINGLE LONGWALL PANEL MODEL WITH NO RIVER VALLEY

; Model based on Metropolitan Colliery
; Using symmetry
; Depth of cover = 413 m
; Longwall width = 105 m
; Extracted thickness = 2.7 m
; W/h ratio = 0.25
; Model dimensions: 815 m x 509.8 m

ti

Model 1 (Metropolitan Colliery)

; Creating model geometry

ro = 0.01

se ov = 0.2

bl 0, -509.8 0, 0 815, 0 815, -509.8

cr 0, -88	815, -88	; Hawkesbury Sandstone (88 m thick)
cr 0, -108	815, -108	; Newport Formation (20 m thick)
cr 0, -142	815, -142	; Bald Hill Claystone (34 m thick)
cr 0, -287	815, -287	; Bulgo Sandstone (145 m thick)
cr 0, -327	815, -327	; Stanwell Park Claystone (40 m thick)
cr 0, -377	815, -377	; Scarborough Sandstone (50 m thick)
cr 0, -393	815, -393	; Wombarra Shale (16 m thick)
cr 0, -413	815, -413	; Coal Cliff Sandstone (20 m thick)
cr 0, -415.7	815, -415.7	; Bulli Seam (2.7 m thick)
cr 0, -423.7	815, -423.7	; Loddon Sandstone (8 m thick)
cr 0, -424.7	815, -424.7	; Balgownie Seam (1 m thick)
cr 0, -428.7	815, -428.7	; Lawrence Sandstone (4 m thick)
cr 0, -430.7	815, -430.7	; Cape Horn Seam (2 m thick)
cr 0, -436.7	815, -436.7	; UN2 (6 m thick)
cr 0, -436.8	815, -436.8	; Hargraves Coal Member (0.1 m thick)
cr 0, -446.8	815, -446.8	; UN3 (10 m thick)
cr 0, -456.8	815, -456.8	; Wongawilli Seam (10 m thick)

Appendix B
Single Longwall Panel Model With No River Valley

cr 0,-459.8 815,-459.8 ; Kembla Sandstone (3 m thick)
cr 0,-509.8 815,-509.8 ; Coal Measures (50 m thick)

; *Defining longwall*

cr 762.5,-413 762.5,-415.7
cr 815,-413 815,-415.7

; *Defining discontinuities*

jr 0,-88 0,0 815,0 815,-88 ; Hawkesbury Sandstone
js 0,0 815,0 0,0 9,0
js 90,0 9,0 9,0 9,0
js 90,0 9,0 9,0 9,0 4.5 -9

jr 0,-108 0,-88 815,-88 815,-108 ; Newport Formation
js 0,0 815,0 0,0 1,0
js 90,0 1,0 1,0 1,0
js 90,0 1,0 1,0 1,0 0.5,-89

jr 0,-142 0,-108 815,-108 815,-142 ; Bald Hill Claystone
js 0,0 815,0 0,0 1,0
js 90,0 1,0 1,0 1,0
js 90,0 1,0 1,0 1,0 0.5,-109

jr 0,-287 0,-142 815,-142 815,-287 ; Bulgo Sandstone
js 0,0 815,0 0,0 9,0
js 90,0 9,0 9,0 9,0
js 90,0 9,0 9,0 9,0 4.5,-153

jr 0,-327 0,-287 815,-287 815,-327 ; Stanwell Park Claystone
js 0,0 815,0 0,0 3,0
js 90,0 3,0 3,0 3,0
js 90,0 3,0 3,0 3,0 1.5,-291

jr 0,-377 0,-327 815,-327 815,-377 ; Scarborough Sandstone
js 0,0 815,0 0,0 4,0
js 90,0 4,0 4,0 4,0
js 90,0 4,0 4,0 4,0 2,-332

Appendix B
Single Longwall Panel Model With No River Valley

```
jr 0,-393 0,-377 815,-377 815,-393 ; Wombarra Shale
js 0,0 815,0 0,0 3,0
js 90,0 3,0 3,0 3,0
js 90,0 3,0 3,0 3,0 1.5,-381
```

```
jr 0,-413 0,-393 815,-393 815,-413 ; Coal Cliff Sandstone
js 0,0 815,0 0,0 3,0
js 90,0 3,0 3,0 3,0
js 90,0 3,0 3,0 3,0 1.5,-399
```

; Generating zones for deformable blocks

```
ge q 12.7 ra 0 815 -88 0 ; Hawkesbury Sandstone
ge q 1.4 ra 0 815 -108 -88 ; Newport Formation
ge q 1.4 ra 0 815 -142 -108 ; Bald Hill Claystone
ge q 12.7 ra 0 815 -287 -142 ; Bulgo Sandstone
ge q 4.2 ra 0 815 -327 -287 ; Stanwell Park Claystone
ge q 5.7 ra 0 815 -377 -327 ; Scarborough Sandstone
ge q 4.2 ra 0 815 -393 -377 ; Wombarra Shale
ge q 4.2 ra 0 815 -413 -393 ; Coal Cliff Sandstone
ge q 3.5 ra 0 815 -415.7 -413 ; Bulli Seam
ge q 11.3 ra 0 815 -423.7 -415.7 ; Loddon Sandstone
ge q 1.4 ra 0 815 -424.7 -423.7 ; Balgownie Seam
ge q 5.7 ra 0 815 -428.7 -424.7 ; Lawrence Sandstone
ge q 2.8 ra 0 815 -430.7 -428.7 ; Cape Horn Seam
ge q 8.5 ra 0 815 -436.7 -430.7 ; UN2
ge q 0.1 ra 0 815 -436.8 -436.7 ; Hargraves Coal Member
ge q 14.1 ra 0 815 -446.8 -436.8 ; UN3
ge q 14.1 ra 0 815 -456.8 -446.8 ; Wongawilli Seam
ge q 4.2 ra 0 815 -459.8 -456.8 ; Kembbla Sandstone
ge q 4.2 ra 0 815 -509.8 -459.8 ; Coal Measures
```

```
sa modell1_ini1.sav
```

; Defining material properties

```
pro m 1 de = 2397 b = 11.47e9 sh = 5.65e9 coh = 9.70e6 fr = 37.25 &
      ten = 3.58e6 ; Hawkesbury Sandstone
```

```
pro m 2 de = 2290 b = 7.77e9 sh = 4.66e9 coh = 8.85e6 fr = 35.00 &
      ten = 3.40e6 ; Newport Formation
```

Appendix B
Single Longwall Panel Model With No River Valley

pro m 3 de = 2719 b = 14.12e9 sh = 4.72e9 coh = 10.60e6 fr = 27.80 &
ten = 2.90e6 ; Bald Hill Claystone

pro m 4 de = 2527 b = 12.60e9 sh = 7.91e9 coh = 17.72e6 fr = 35.40 &
ten = 6.55e6 ; Bulgo Sandstone

pro m 5 de = 2693 b = 13.22e9 sh = 7.63e9 coh = 14.57e6 fr = 27.80 &
ten = 4.83e6 ; Stanwell Park Claystone

pro m 6 de = 2514 b = 16.16e9 sh = 10.80e9 coh = 13.25e6 fr = 40.35 &
ten = 7.18e6 ; Scarborough Sandstone

pro m 7 de = 2643 b = 24.81e9 sh = 7.24e9 coh = 14.51e6 fr = 27.80 &
ten = 4.81e6 ; Wombarra Shale

pro m 8 de = 2600 b = 17.07e9 sh = 11.44e9 coh = 19.40e6 fr = 33.30 &
ten = 7.87e6 ; Coal Cliff Sandstone

pro m 9 de = 1500 b = 2.33e9 sh = 1.08e9 coh = 6.37e6 fr = 25.00 &
ten = 0.84e6 ; Bulli Seam

pro m 10 de = 2539 b = 16.76e9 sh = 6.51e9 coh = 17.10e6 fr = 28.90 &
ten = 5.65e6 ; Loddon Sandstone

pro m 11 de = 1500 b = 2.33e9 sh = 1.08e9 coh = 6.37e6 fr = 25.00 &
ten = 0.84e6 ; Balgownie Seam

pro m 12 de = 2539 b = 16.76e9 sh = 6.51e9 coh = 17.10e6 fr = 28.90 &
ten = 5.65e6 ; Lawrence Sandstone

pro m 13 de = 1500 b = 1.67e9 sh = 0.77e9 coh = 2.87e6 fr = 25.00 &
ten = 0.70e6 ; Cape Horn Seam

pro m 14 de = 2560 b = 8.99e9 sh = 5.39e9 coh = 19.89e6 fr = 28.90 &
ten = 6.74e6 ; UN2

pro m 15 de = 1500 b = 2.33e9 sh = 1.08e9 coh = 6.37e6 fr = 25.00 &
ten = 0.84e6 ; Hargraves Coal Member

pro m 16 de = 2620 b = 8.67e9 sh = 5.20e9 coh = 19.18e6 fr = 28.90 &
ten = 6.50e6 ; UN3

Appendix B
Single Longwall Panel Model With No River Valley

pro m 17 de = 1500 b = 1.67e9 sh = 0.77e9 coh = 2.87e6 fr = 25.00 &
ten = 0.70e6 ; Wongawilli Seam

pro m 18 de = 2569 b = 13.79e9 sh = 7.12e9 coh = 18.02e6 fr = 28.90 &
ten = 6.11e6 ; Kembla Sandstone

pro m 19 de = 2092 b = 8.11e9 sh = 3.83e9 coh = 12.20e6 fr = 27.17 &
ten = 3.75e6 ; Coal Measures

; Assigning material properties

ch cons 3

ch m 1 ra 0 815 -88 0 ; Hawkesbury Sandstone
ch m 2 ra 0 815 -108 -88 ; Newport Formation
ch m 3 ra 0 815 -142 -108 ; Bald Hill Claystone
ch m 4 ra 0 815 -287 -142 ; Bulgo Sandstone
ch m 5 ra 0 815 -327 -287 ; Stanwell Park Claystone
ch m 6 ra 0 815 -377 -327 ; Scarborough Sandstone
ch m 7 ra 0 815 -393 -377 ; Wombarra Shale
ch m 8 ra 0 815 -413 -393 ; Coal Cliff Sandstone
ch m 9 ra 0 815 -415.7 -413 ; Bulli Seam
ch m 10 ra 0 815 -423.7 -415.7 ; Loddon Sandstone
ch m 11 ra 0 815 -424.7 -423.7 ; Balgownie Seam
ch m 12 ra 0 815 -428.7 -424.7 ; Lawrence Sandstone
ch m 13 ra 0 815 -430.7 -428.7 ; Cape Horn Seam
ch m 14 ra 0 815 -436.7 -430.7 ; UN2
ch m 15 ra 0 815 -436.8 -436.7 ; Hargraves Coal Member
ch m 16 ra 0 815 -446.8 -436.8 ; UN3
ch m 17 ra 0 815 -456.8 -446.8 ; Wongawilli Seam
ch m 18 ra 0 815 -459.8 -456.8 ; Kembla Sandstone
ch m 19 ra 0 815 -509.8 -459.8 ; Coal Measures

; Defining bedding plane properties

pro jm = 1 jkn = 21e9 jks = 2.1e9 & ; Hawkesbury Sandstone
j f = 25 jrf = 15 &
j c = 0.29e6 jresc = 0

Appendix B
Single Longwall Panel Model With No River Valley

```
pro jm = 2 jkn = 140e9 jks = 14e9 & ; Newport Formation
          jf = 25      jrf = 15    &
          jc = 0.29e6 jresc = 0

pro jm = 3 jkn = 204e9 jks = 20.4e9 & ; Bald Hill Claystone
          jf = 25      jrf = 15    &
          jc = 0.29e6 jresc = 0

pro jm = 4 jkn = 26e9  jks = 2.6e9  & ; Bulgo Sandstone
          jf = 25      jrf = 15    &
          jc = 0.29e6 jresc = 0

pro jm = 5 jkn = 78e9  jks = 7.8e9  & ; Stanwell Park Claystone
          jfc = 25     jrf = 15    &
          jc = 0.29e6 jresc = 0

pro jm = 6 jkn = 76e9  jks = 7.6e9  & ; Scarborough Sandstone
          jf = 25      jrf = 15    &
          jc = 0.29e6 jresc = 0

pro jm = 7 jkn = 115e9 jks = 11.5e9 & ; Wombarra Shale
          jf = 25      jrf = 15    &
          jc = 0.29e6 jresc = 0

pro jm = 8 jkn = 400e9 jks = 40e9   & ; Coal Cliff Sandstone
          jf = 25      jrf = 15    &
          jc = 0.29e6 jresc = 0

pro jm = 9 jkn = 400e9 jks = 40e9   & ; Sub Bulli
          jf = 25      jrf = 15    &
          jc = 0.29e6 jresc = 0
```

; Assigning bedding plane properties

```
ch jc = 5 ra 0 815 -509.8 0 ang -1 1
se jc = 5
```

```
ch jm 1 ra 0 815 -88 0 ang -1 1 ; Hawkesbury Sandstone
ch jm 2 ra 0 815 -108 -88 ang -1 1 ; Newport Formation
ch jm 3 ra 0 815 -142 -108 ang -1 1 ; Bald Hill Claystone
ch jm 4 ra 0 815 -287 -142 ang -1 1 ; Bulgo Sandstone
```

Appendix B
Single Longwall Panel Model With No River Valley

ch jm 5 ra 0 815 -327 -287 ang -1 1 ; Stanwell Park Claystone
ch jm 6 ra 0 815 -377 -327 ang -1 1 ; Scarborough Sandstone
ch jm 7 ra 0 815 -393 -377 ang -1 1 ; Wombarra Shale
ch jm 8 ra 0 815 -413 -393 ang -1 1 ; Coal Cliff Sandstone
ch jm 9 ra 0 815 -509.8 -413 ang -1 1 ; Sub Bulli

; Defining vertical joint properties

pro jm = 10 jkn = 21e9 jks = 2.1e9 & ; Hawkesbury Sandstone
jf = 19 jrf = 15 &
jc = 0.86e6 jresc = 0

pro jm = 11 jkn = 140e9 jks = 14e9 & ; Newport Formation
jf = 19 jrf = 15 &
jc = 0.86e6 jresc = 0

pro jm = 12 jkn = 204e9 jks = 20.4e9 & ; Bald Hill Claystone
jf = 19 jrf = 15 &
jc = 0.86e6 jresc = 0

pro jm = 13 jkn = 26e9 jks = 2.6e9 & ; Bulgo Sandstone
jf = 19 jrf = 15 &
jc = 0.86e6 jresc = 0

pro jm = 14 jkn = 78e9 jks = 7.8e9 & ; Stanwell Park Claystone
jf = 19 jrf = 15 &
jc = 0.86e6 jresc = 0

pro jm = 15 jkn = 76e9 jks = 7.6e9 & ; Scarborough Sandstone
jf = 19 jrf = 15 &
jc = 0.86e6 jresc = 0

pro jm = 16 jkn = 115e9 jks = 11.5e9 & ; Wombarra Shale
jf = 19 jrf = 15 &
jc = 0.86e6 jresc = 0

pro jm = 17 jkn = 400e9 jks = 40e9 & ; Coal Cliff Sandstone
jf = 19 jrf = 15 &
jc = 0.86e6 jresc = 0

Appendix B
Single Longwall Panel Model With No River Valley

```
pro jm = 18 jkn = 400e9 jks = 40e9 & ; Sub Bulli
      jf = 19 jrf = 15 &
      jc = 0.86e6 jresc = 0

; Assigning vertical joint properties

ch jc = 5 ra 0 815 -509.8 0 ang 89 91
se jc = 5

ch jm 10 ra 0 815 -88 0 ang 89 91 ; Hawkesbury Sandstone
ch jm 11 ra 0 815 -108 -88 ang 89 91 ; Newport Formation
ch jm 12 ra 0 815 -142 -108 ang 89 91 ; Bald Hill Claystone
ch jm 13 ra 0 815 -287 -142 ang 89 91 ; Bulgo Sandstone
ch jm 14 ra 0 815 -327 -287 ang 89 91 ; Stanwell Park Claystone
ch jm 15 ra 0 815 -377 -327 ang 89 91 ; Scarborough Sandstone
ch jm 16 ra 0 815 -393 -377 ang 89 91 ; Wombarra Shale
ch jm 17 ra 0 815 -413 -393 ang 89 91 ; Coal Cliff Sandstone
ch jm 18 ra 0 815 -509.8 -413 ang 89 91 ; Sub Bulli

; Defining gravity

se gr 0 -9.81

; Defining boundary conditions

bo xv 0 ra -0.1 0.1 -509.8 0
bo xv 0 ra 814.9 815.1 -509.8,0
bo yv 0 ra 0 815 -509.9 -509.7

; Defining initial stress conditions

in st 0 0 0 yg 4.82e4 0 2.41e4 szz 0 zg 0 4.82e4 ra 0 815 -509.8 0

da a

so

sa modell1_ini2.sav
```

Appendix B
Single Longwall Panel Model With No River Valley

; Initialising displacements

rese vel

rese di

; Defining histories

; Y-displacements

hi yd 0 0 ;1

hi yd 4.5 0 ;2

hi yd 13.5 0 ;3

hi yd 22.5 0 ;4

hi yd 31.5 0 ;5

hi yd 40.5 0 ;6

hi yd 49.5 0 ;7

hi yd 58.5 0 ;8

hi yd 67.5 0 ;9

hi yd 76.5 0 ;10

hi yd 85.5 0 ;11

hi yd 94.5 0 ;12

hi yd 103.5 0 ;13

hi yd 112.5 0 ;14

hi yd 121.5 0 ;15

hi yd 130.5 0 ;16

hi yd 139.5 0 ;17

hi yd 148.5 0 ;18

hi yd 157.5 0 ;19

hi yd 166.5 0 ;20

hi yd 175.5 0 ;21

hi yd 184.5 0 ;22

hi yd 193.5 0 ;23

hi yd 202.5 0 ;24

hi yd 211.5 0 ;25

hi yd 220.5 0 ;26

hi yd 229.5 0 ;27

hi yd 238.5 0 ;28

hi yd 247.5 0 ;29

hi yd 256.5 0 ;30

hi yd 265.5 0 ;31

hi yd 274.5 0 ;32

hi yd 283.5 0 ;33

Appendix B
Single Longwall Panel Model With No River Valley

hi yd 292.5 0 ;34
hi yd 301.5 0 ;35
hi yd 310.5 0 ;36
hi yd 319.5 0 ;37
hi yd 328.5 0 ;38
hi yd 337.5 0 ;39
hi yd 346.5 0 ;40
hi yd 355.5 0 ;41
hi yd 364.5 0 ;42
hi yd 373.5 0 ;43
hi yd 382.5 0 ;44
hi yd 391.5 0 ;45
hi yd 400.5 0 ;46
hi yd 409.5 0 ;47
hi yd 418.5 0 ;48
hi yd 427.5 0 ;49
hi yd 436.5 0 ;50
hi yd 445.5 0 ;51
hi yd 454.5 0 ;52
hi yd 463.5 0 ;53
hi yd 472.5 0 ;54
hi yd 481.5 0 ;55
hi yd 490.5 0 ;56
hi yd 499.5 0 ;57
hi yd 508.5 0 ;58
hi yd 517.5 0 ;59
hi yd 526.5 0 ;60
hi yd 535.5 0 ;61
hi yd 544.5 0 ;62
hi yd 553.5 0 ;63
hi yd 562.5 0 ;64
hi yd 571.5 0 ;65
hi yd 580.5 0 ;66
hi yd 589.5 0 ;67
hi yd 598.5 0 ;68
hi yd 607.5 0 ;69
hi yd 616.5 0 ;70
hi yd 625.5 0 ;71
hi yd 634.5 0 ;72
hi yd 643.5 0 ;73
hi yd 652.5 0 ;74

Appendix B
Single Longwall Panel Model With No River Valley

hi yd 661.5 0 ;75
hi yd 670.5 0 ;76
hi yd 679.5 0 ;77
hi yd 688.5 0 ;78
hi yd 697.5 0 ;79
hi yd 706.5 0 ;80
hi yd 715.5 0 ;81
hi yd 724.5 0 ;82
hi yd 733.5 0 ;83
hi yd 742.5 0 ;84
hi yd 751.5 0 ;85
hi yd 760.5 0 ;86
hi yd 769.5 0 ;87
hi yd 778.5 0 ;88
hi yd 787.5 0 ;89
hi yd 796.5 0 ;90
hi yd 805.5 0 ;91
hi yd 814.5 0 ;92
hi yd 815.0 0 ;93

; X-displacements

hi xd 0 0 ;94
hi xd 4.5 0 ;95
hi xd 13.5 0 ;96
hi xd 22.5 0 ;97
hi xd 31.5 0 ;98
hi xd 40.5 0 ;99
hi xd 49.5 0 ;100
hi xd 58.5 0 ;101
hi xd 67.5 0 ;102
hi xd 76.5 0 ;103
hi xd 85.5 0 ;104
hi xd 94.5 0 ;105
hi xd 103.5 0 ;106
hi xd 112.5 0 ;107
hi xd 121.5 0 ;108
hi xd 130.5 0 ;109
hi xd 139.5 0 ;110
hi xd 148.5 0 ;111
hi xd 157.5 0 ;112

Appendix B
Single Longwall Panel Model With No River Valley

hi xd 166.5 0 ;113
hi xd 175.5 0 ;114
hi xd 184.5 0 ;115
hi xd 193.5 0 ;116
hi xd 202.5 0 ;117
hi xd 211.5 0 ;118
hi xd 220.5 0 ;119
hi xd 229.5 0 ;120
hi xd 238.5 0 ;121
hi xd 247.5 0 ;122
hi xd 256.5 0 ;123
hi xd 265.5 0 ;124
hi xd 274.5 0 ;125
hi xd 283.5 0 ;126
hi xd 292.5 0 ;127
hi xd 301.5 0 ;128
hi xd 310.5 0 ;129
hi xd 319.5 0 ;130
hi xd 328.5 0 ;131
hi xd 337.5 0 ;132
hi xd 346.5 0 ;133
hi xd 355.5 0 ;134
hi xd 364.5 0 ;135
hi xd 373.5 0 ;136
hi xd 382.5 0 ;137
hi xd 391.5 0 ;138
hi xd 400.5 0 ;139
hi xd 409.5 0 ;140
hi xd 418.5 0 ;141
hi xd 427.5 0 ;142
hi xd 436.5 0 ;143
hi xd 445.5 0 ;144
hi xd 454.5 0 ;145
hi xd 463.5 0 ;146
hi xd 472.5 0 ;147
hi xd 481.5 0 ;148
hi xd 490.5 0 ;149
hi xd 499.5 0 ;150
hi xd 508.5 0 ;151
hi xd 517.5 0 ;152
hi xd 526.5 0 ;153

Appendix B
Single Longwall Panel Model With No River Valley

hi xd 535.5 0 ;154
hi xd 544.5 0 ;155
hi xd 553.5 0 ;156
hi xd 562.5 0 ;157
hi xd 571.5 0 ;158
hi xd 580.5 0 ;159
hi xd 589.5 0 ;160
hi xd 598.5 0 ;161
hi xd 607.5 0 ;162
hi xd 616.5 0 ;163
hi xd 625.5 0 ;164
hi xd 634.5 0 ;165
hi xd 643.5 0 ;166
hi xd 652.5 0 ;167
hi xd 661.5 0 ;168
hi xd 670.5 0 ;169
hi xd 679.5 0 ;170
hi xd 688.5 0 ;171
hi xd 697.5 0 ;172
hi xd 706.5 0 ;173
hi xd 715.5 0 ;174
hi xd 724.5 0 ;175
hi xd 733.5 0 ;176
hi xd 742.5 0 ;177
hi xd 751.5 0 ;178
hi xd 760.5 0 ;179
hi xd 769.5 0 ;180
hi xd 778.5 0 ;181
hi xd 787.5 0 ;182
hi xd 796.5 0 ;183
hi xd 805.5 0 ;184
hi xd 814.5 0 ;185
hi xd 815.0 0 ;186
hi u ;187

; Extracting longwall - instantaneous extraction

de b 4098

da a

; Solving for equilibrium

so rat 1e-5 ste 1000000000

sa modell_final.sav

APPENDIX C

RIVER VALLEY MODEL WITH PLANE AT BASE

ti

Valley 1

; Creating model geometry

ro = 0.01

set ov = 0.2

bl 0,-189 0,0 1050,0 1050,-189

cr 0,-78 1050,-78 ; Hawkesbury Sandstone (78 m thick)

cr 0,-85 1050,-85 ; Newport Formation (7 m thick)

cr 0,-97 1050,-97 ; Bald Hill Claystone (9 m thick)

cr 0,-186 1050,-186 ; Bulgo Sandstone (89 m thick + 3 m thick beam)

; Generating vertical cracks for beam at base of Bald Hill Claystone

jr 0,-189 0,-186 525,-186 525,-189

js 90,0 3,0 0,0 9,0 13.5,-189

cr 525,-189 525,-186

cr 532.5,-189 532.5,-186

jr 532.5,-189 532.5,-186 1050,-186 1050,-189

js 90,0 3,0 0,0 9,0 1045.5,-189

; Generating pre-defined cracks for valleys (70 m deep x 50 m wide)

cr 0,-70 1050,-70

cr 500,-70 500,0

cr 450,-70 450,0

cr 400,-70 400,0

cr 350,-70 350,0

cr 300,-70 300,0

cr 250,-70 250,0

cr 200,-70 200,0

cr 150,-70 150,0

cr 100,-70 100,0

Appendix C
River Valley Model With Plane At Base

cr 50,-70 50,0
cr 550,-70 550,0
cr 600,-70 600,0
cr 650,-70 650,0
cr 700,-70 700,0
cr 750,-70 750,0
cr 800,-70 800,0
cr 850,-70 850,0
cr 900,-70 900,0
cr 950,-70 950,0
cr 1000,-70 1000,0

; Defining discontinuities

jr 0,-78 0,-70 1050,-70 1050,-78 ; Hawkesbury Sandstone
js 90,0 9,0 9,0 9,0 4.5 -78

jr 0,-85 0,-78 1050,-78 1050,-85 ; Newport Formation
js 0,0 1050,0 0,0 1,0
js 90,0 1,0 1,0 1,0
js 90,0 1,0 1,0 1,0 0.5,-79

jr 0,-97 0,-85 1050,-85 1050,-97 ; Bald Hill Claystone
js 0,0 1050,0 0,0 1,0
js 90,0 1,0 1,0 1,0
js 90,0 1,0 1,0 1,0 0.5,-87

jr 0,-186 0,-97 1050,-97 1050,-186 ; Bulgo Sandstone
js 0,0 525,0 0,0 9,0
js 90,0 9,0 9,0 9,0
js 90,0 9,0 9,0 9,0 4.5,-117
jr 0,-189 0,-186 525,-186 525,-189
js 90,0 3,0 0,0 9,0 13.5,-189
cr 525,-189 525,-186
cr 532.5,-189 532.5,-186
jr 532.5,-189 532.5,-186 1050,-186 1050,-189
js 90,0 3,0 0,0 9,0 1045.5,-189

Appendix C
River Valley Model With Plane At Base

; Generating zones for deformable blocks

ge q 12.7 ra 0 1050 -78 0 ; Hawkesbury Sandstone
ge q 1.4 ra 0 1050 -85 -78 ; Newport Formation
ge q 1.4 ra 0 1050 -97 -85 ; Bald Hill Claystone
ge q 12.7 ra 0 1050 -189 -97 ; Bulgo Sandstone

; Defining material properties

pro m 1 de = 2397 b = 11.47e9 sh = 5.65e9 coh = 9.70e6 fr= 37.25 &
ten = 3.58e6 ; Hawkesbury Sandstone

pro m 2 de = 2290 b = 7.77e9 sh = 4.66e9 coh = 8.85e6 fr= 35.00 &
ten = 3.40e6 ; Newport Formation

pro m 3 de = 2719 b = 14.12e9 sh = 4.72e9 coh = 10.60e6 fr= 27.80 &
ten = 2.90e6 ; Bald Hill Claystone

pro m 4 de = 2527 b = 12.60e9 sh = 7.91e9 coh = 17.72e6 fr= 35.40 &
ten = 6.55e6 ; Bulgo Sandstone

; Assigning material properties

ch cons 3

ch m 1 ra 0 1050 -78 0 ; Hawkesbury Sandstone
ch m 2 ra 0 1050 -85 -78 ; Newport Formation
ch m 3 ra 0 1050 -97 -85 ; Bald Hill Claystone
ch m 4 ra 0 1050 -189 -97 ; Bulgo Sandstone

; Defining bedding plane properties

pro jm = 1 jkn = 21e9 jks = 2.1e9 & ; Hawkesbury Sandstone
j f = 25 jrf = 15 &
j c = 0.29e6 jresc = 0

pro jm = 2 jkn = 140e9 jks = 14.0e9 & ; Newport Formation
j f = 25 jrf = 15 &
j c = 0.29e6 jresc = 0

Appendix C
River Valley Model With Plane At Base

pro jm = 3 jkn = 204e9 jks = 20.4e9 & ; Bald Hill Claystone
j f = 25 jrf = 15 &
j c = 0.29e6 jresc = 0

pro jm = 4 jkn = 26e9 jks = 2.6e9 & ; Bulgo Sandstone
j f = 25 jrf = 15 &
j c = 0.29e6 jresc = 0

pro jm = 5 jkn = 204e9 jks = 20.4e9 & ; Beam
j f = 89 jrf = 89 &
j c = 1e10 jresc = 1e10 &
j t = 1e10 jrt = 1e10

; Assigning bedding plane properties

ch jc = 5 ra 0 1050 -189 0 ang -1 1
se jc = 5

ch jm 1 ra 0 1050 -78 0 ang -1 1 ; Hawkesbury Sandstone
ch jm 2 ra 0 1050 -85 -78 ang -1 1 ; Newport Formation
ch jm 3 ra 0 1050 -97 -85 ang -1 1 ; Bald Hill Claystone
ch jm 4 ra 0 1050 -186 -97 ang -1 1 ; Bulgo Sandstone
ch jm 5 ra 0 1050 -189 -186 ang -1 1 ; Beam

; Vertical joint properties

pro jm = 6 jkn = 21e9 jks = 2.1e9 & ; Hawkesbury Sandstone
j f = 19 jrf = 15 &
j c = 0.86e6 jresc = 0

pro jm = 7 jkn = 140e9 jks = 14.0e9 & ; Newport Formation
j f = 19 jrf = 15 &
j c = 0.86e6 jresc = 0

pro jm = 8 jkn = 204e9 jks = 20.4e9 & ; Bald Hill Claystone
j f = 19 jrf = 15 &
j c = 0.86e6 jresc = 0

pro jm = 9 jkn = 26e9 jks = 2.6e9 & ; Bulgo Sandstone;
j f = 19 jrf = 15 &
j c = 0.86e6 jresc = 0

Appendix C
River Valley Model With Plane At Base

```
pro jm = 10 jkn = 204e9 jks = 20.4e9 & ; Beam
      jf = 89 jrf = 89 &
      jc = 1e10 jresc = 1e10 &
      jt = 1e10 jrt = 1e10
```

; Assigning vertical joint properties

```
ch jc = 5 ra 0 1050 -189 0 ang 89 91
se jc = 5
```

```
ch jm 6 ra 0 1050 -186 0 ang 89 91 ; Hawkesbury Sandstone
ch jm 7 ra 0 1050 -85 -78 ang 89 91 ; Newport Formation
ch jm 8 ra 0 1050 -97 -85 ang 89 91 ; Bald Hill Claystone
ch jm 9 ra 0 1050 -186 -97 ang 89 91 ; Bulgo Sandstone
ch jm 10 ra 0 1050 -189 -186 ang 89 91 ; Beam
```

; Defining gravity

```
se gr 0 -9.81
```

; Defining boundary conditions

```
bo yv 0 ra 0 1050 -189.1 -188.9
bo xv 0 ra -0.1 0.1 -189.1 0.1
bo xv 0 ra 1049.9 1050.1 -189.1 0.1
```

; Defining initial stress conditions

```
in st 0 0 0 yg 4.77e4 0 2.39e4 szz 0 zg 0 4.77e4 ra 0 1050 -189 0
```

```
sa valley1_ini1.sav
```

; Cycle to equilibrium

```
da a
```

```
so
```

Appendix C
River Valley Model With Plane At Base

; Removing valley and cycle to equilibrium

de ra 500 550 -70 0

da a

so

; Removing boundary conditions at base and attaching pre-determined y-displacements

rese vel

rese di

bo yfr

bo xfr

bo xv 0 ra -0.1 0.1 -189.1 0.1

bo xv 0 ra 1049.9 1050.1 -189.1 0.1

; Histories

; X Displacements (valley closure)

; Top of valley

hi xd 50 0 ;1

hi xd 100 0 ;2

hi xd 150 0 ;3

hi xd 200 0 ;4

hi xd 250 0 ;5

hi xd 300 0 ;6

hi xd 350 0 ;7

hi xd 400 0 ;8

hi xd 450 0 ;9

hi xd 500 0 ;10

hi xd 550 0 ;11

; Y Displacements (subsidence)

hi yd 0 0 ;12

hi yd 25 0 ;13

hi yd 50 0 ;14

Appendix C
River Valley Model With Plane At Base

hi yd 75 0 ;15
hi yd 100 0 ;16
hi yd 125 0 ;17
hi yd 150 0 ;18
hi yd 175 0 ;19
hi yd 200 0 ;20
hi yd 225 0 ;21
hi yd 250 0 ;22
hi yd 275 0 ;23
hi yd 300 0 ;24
hi yd 325 0 ;25
hi yd 350 0 ;26
hi yd 375 0 ;27
hi yd 400 0 ;28
hi yd 425 0 ;29
hi yd 450 0 ;30
hi yd 475 0 ;31
hi yd 500 0 ;32
hi yd 525 0 ;33
hi yd 550 0 ;34
hi yd 575 0 ;35
hi yd 600 0 ;36
hi yd 625 0 ;37
hi yd 650 0 ;38
hi yd 675 0 ;39
hi yd 700 0 ;40
hi yd 725 0 ;41
hi yd 750 0 ;42
hi yd 775 0 ;43
hi yd 800 0 ;44
hi yd 825 0 ;45
hi yd 850 0 ;46
hi yd 875 0 ;47
hi yd 900 0 ;48
hi yd 925 0 ;49
hi yd 950 0 ;50
hi yd 975 0 ;51
hi yd 1000 0 ;52
hi yd 1025 0 ;53
hi yd 1050 0 ;54

Appendix C
River Valley Model With Plane At Base

; Y displacements (base)

hi yd 0 -189 ;55
hi yd 4.5 -189 ;56
hi yd 13.5 -189 ;57
hi yd 22.5 -189 ;58
hi yd 31.5 -189 ;59
hi yd 40.5 -189 ;60
hi yd 49.5 -189 ;61
hi yd 58.5 -189 ;62
hi yd 67.5 -189 ;63
hi yd 76.5 -189 ;64
hi yd 85.5 -189 ;65
hi yd 94.5 -189 ;66
hi yd 103.5 -189 ;67
hi yd 112.5 -189 ;68
hi yd 121.5 -189 ;69
hi yd 130.5 -189 ;70
hi yd 139.5 -189 ;71
hi yd 148.5 -189 ;72
hi yd 157.5 -189 ;73
hi yd 166.5 -189 ;74
hi yd 175.5 -189 ;75
hi yd 184.5 -189 ;76
hi yd 193.5 -189 ;77
hi yd 202.5 -189 ;78
hi yd 211.5 -189 ;79
hi yd 220.5 -189 ;80
hi yd 229.5 -189 ;81
hi yd 238.5 -189 ;82
hi yd 247.5 -189 ;83
hi yd 256.5 -189 ;84
hi yd 265.5 -189 ;85
hi yd 274.5 -189 ;86
hi yd 283.5 -189 ;87
hi yd 292.5 -189 ;88
hi yd 301.5 -189 ;89
hi yd 310.5 -189 ;90
hi yd 319.5 -189 ;91
hi yd 328.5 -189 ;92
hi yd 337.5 -189 ;93

```
hi yd 346.5 -189 ;94
hi yd 355.5 -189 ;95
hi yd 364.5 -189 ;96
hi yd 373.5 -189 ;97
hi yd 382.5 -189 ;98
hi yd 391.5 -189 ;99
hi yd 400.5 -189 ;100
hi yd 409.5 -189 ;101
hi yd 418.5 -189 ;102
hi yd 427.5 -189 ;103
hi yd 436.5 -189 ;104
hi yd 445.5 -189 ;105
hi yd 454.5 -189 ;106
hi yd 463.5 -189 ;107
hi yd 472.5 -189 ;108
hi yd 481.5 -189 ;109
hi yd 490.5 -189 ;110
hi yd 499.5 -189 ;111
hi yd 508.5 -189 ;112
hi yd 517.5 -189 ;113
hi yd 525.0 -189 ;114
```

; Creating y-velocities at base and final solving routine

```
def valleysolve
```

; Step 1 to obtain time step

```
command
```

```
cyc 1
```

```
end_command
```

; Identifying gridpoints at base to which velocities will be attached

```
gri_chk1 = gp_near(0.0, -189)
gri_chk2 = gp_near(4.5, -189)
gri_chk3 = gp_near(13.5, -189)
gri_chk4 = gp_near(22.5, -189)
gri_chk5 = gp_near(31.5, -189)
gri_chk6 = gp_near(40.5, -189)
gri_chk7 = gp_near(49.5, -189)
```

Appendix C
River Valley Model With Plane At Base

gri_chk8 = gp_near(58.5, -189)
gri_chk9 = gp_near(67.5, -189)
gri_chk10 = gp_near(76.5, -189)
gri_chk11 = gp_near(85.5, -189)
gri_chk12 = gp_near(94.5, -189)
gri_chk13 = gp_near(103.5, -189)
gri_chk14 = gp_near(112.5, -189)
gri_chk15 = gp_near(121.5, -189)
gri_chk16 = gp_near(130.5, -189)
gri_chk17 = gp_near(139.5, -189)
gri_chk18 = gp_near(148.5, -189)
gri_chk19 = gp_near(157.5, -189)
gri_chk20 = gp_near(166.5, -189)
gri_chk21 = gp_near(175.5, -189)
gri_chk22 = gp_near(184.5, -189)
gri_chk23 = gp_near(193.5, -189)
gri_chk24 = gp_near(202.5, -189)
gri_chk25 = gp_near(211.5, -189)
gri_chk26 = gp_near(220.5, -189)
gri_chk27 = gp_near(229.5, -189)
gri_chk28 = gp_near(238.5, -189)
gri_chk29 = gp_near(247.5, -189)
gri_chk30 = gp_near(256.5, -189)
gri_chk31 = gp_near(265.5, -189)
gri_chk32 = gp_near(274.5, -189)
gri_chk33 = gp_near(283.5, -189)
gri_chk34 = gp_near(292.5, -189)
gri_chk35 = gp_near(301.5, -189)
gri_chk36 = gp_near(310.5, -189)
gri_chk37 = gp_near(319.5, -189)
gri_chk38 = gp_near(328.5, -189)
gri_chk39 = gp_near(337.5, -189)
gri_chk40 = gp_near(346.5, -189)
gri_chk41 = gp_near(355.5, -189)
gri_chk42 = gp_near(364.5, -189)
gri_chk43 = gp_near(373.5, -189)
gri_chk44 = gp_near(382.5, -189)
gri_chk45 = gp_near(391.5, -189)
gri_chk46 = gp_near(400.5, -189)
gri_chk47 = gp_near(409.5, -189)
gri_chk48 = gp_near(418.5, -189)

Appendix C
River Valley Model With Plane At Base

gri_chk49 = gp_near(427.5, -189)
gri_chk50 = gp_near(436.5, -189)
gri_chk51 = gp_near(445.5, -189)
gri_chk52 = gp_near(454.5, -189)
gri_chk53 = gp_near(463.5, -189)
gri_chk54 = gp_near(472.5, -189)
gri_chk55 = gp_near(481.5, -189)
gri_chk56 = gp_near(490.5, -189)
gri_chk57 = gp_near(499.5, -189)
gri_chk58 = gp_near(508.5, -189)
gri_chk59 = gp_near(517.5, -189)
gri_chk60 = gp_near(525.0, -189)
gri_chk61 = gp_near(532.5, -189)
gri_chk62 = gp_near(541.5, -189)
gri_chk63 = gp_near(550.5, -189)
gri_chk64 = gp_near(559.5, -189)
gri_chk65 = gp_near(568.5, -189)
gri_chk66 = gp_near(577.5, -189)
gri_chk67 = gp_near(586.5, -189)
gri_chk68 = gp_near(595.5, -189)
gri_chk69 = gp_near(604.5, -189)
gri_chk70 = gp_near(613.5, -189)
gri_chk71 = gp_near(622.5, -189)
gri_chk72 = gp_near(631.5, -189)
gri_chk73 = gp_near(640.5, -189)
gri_chk74 = gp_near(649.5, -189)
gri_chk75 = gp_near(658.5, -189)
gri_chk76 = gp_near(667.5, -189)
gri_chk77 = gp_near(676.5, -189)
gri_chk78 = gp_near(685.5, -189)
gri_chk79 = gp_near(694.5, -189)
gri_chk80 = gp_near(703.5, -189)
gri_chk81 = gp_near(712.5, -189)
gri_chk82 = gp_near(721.5, -189)
gri_chk83 = gp_near(730.5, -189)
gri_chk84 = gp_near(739.5, -189)
gri_chk85 = gp_near(748.5, -189)
gri_chk86 = gp_near(757.5, -189)
gri_chk87 = gp_near(766.5, -189)
gri_chk88 = gp_near(775.5, -189)
gri_chk89 = gp_near(784.5, -189)

Appendix C
River Valley Model With Plane At Base

```
gri_chk90 = gp_near(793.5, -189)
gri_chk91 = gp_near(802.5, -189)
gri_chk92 = gp_near(811.5, -189)
gri_chk93 = gp_near(820.5, -189)
gri_chk94 = gp_near(829.5, -189)
gri_chk95 = gp_near(838.5, -189)
gri_chk96 = gp_near(847.5, -189)
gri_chk97 = gp_near(856.5, -189)
gri_chk98 = gp_near(865.5, -189)
gri_chk99 = gp_near(874.5, -189)
gri_chk100 = gp_near(883.5, -189)
gri_chk101 = gp_near(892.5, -189)
gri_chk102 = gp_near(901.5, -189)
gri_chk103 = gp_near(910.5, -189)
gri_chk104 = gp_near(919.5, -189)
gri_chk105 = gp_near(928.5, -189)
gri_chk106 = gp_near(937.5, -189)
gri_chk107 = gp_near(946.5, -189)
gri_chk108 = gp_near(955.5, -189)
gri_chk109 = gp_near(964.5, -189)
gri_chk110 = gp_near(973.5, -189)
gri_chk111 = gp_near(982.5, -189)
gri_chk112 = gp_near(991.5, -189)
gri_chk113 = gp_near(1000.5, -189)
gri_chk114 = gp_near(1009.5, -189)
gri_chk115 = gp_near(1018.5, -189)
gri_chk116 = gp_near(1027.5, -189)
gri_chk117 = gp_near(1036.5, -189)
gri_chk118 = gp_near(1045.5, -189)
gri_chk119 = gp_near(1050.0, -189)
```

; Defining y-displacements from Model 4

```
max_disp1 = 1.398e-03
max_disp2 = 1.394e-03
max_disp3 = 1.372e-03
max_disp4 = 1.331e-03
max_disp5 = 1.270e-03
max_disp6 = 1.188e-03
max_disp7 = 1.086e-03
max_disp8 = 9.621e-04
```

Appendix C
River Valley Model With Plane At Base

max_disp9 = 8.172e-04
max_disp10 = 6.505e-04
max_disp11 = 4.614e-04
max_disp12 = 2.494e-04
max_disp13 = 1.411e-05
max_disp14 = -2.455e-04
max_disp15 = -5.299e-04
max_disp16 = -8.401e-04
max_disp17 = -1.177e-03
max_disp18 = -1.542e-03
max_disp19 = -1.937e-03
max_disp20 = -2.362e-03
max_disp21 = -2.820e-03
max_disp22 = -3.313e-03
max_disp23 = -3.843e-03
max_disp24 = -4.413e-03
max_disp25 = -5.027e-03
max_disp26 = -5.686e-03
max_disp27 = -6.396e-03
max_disp28 = -7.159e-03
max_disp29 = -7.980e-03
max_disp30 = -8.861e-03
max_disp31 = -9.804e-03
max_disp32 = -1.081e-02
max_disp33 = -1.190e-02
max_disp34 = -1.306e-02
max_disp35 = -1.430e-02
max_disp36 = -1.562e-02
max_disp37 = -1.703e-02
max_disp38 = -1.854e-02
max_disp39 = -2.014e-02
max_disp40 = -2.185e-02
max_disp41 = -2.367e-02
max_disp42 = -2.563e-02
max_disp43 = -2.778e-02
max_disp44 = -3.024e-02
max_disp45 = -3.344e-02
max_disp46 = -3.810e-02
max_disp47 = -4.513e-02
max_disp48 = -5.516e-02
max_disp49 = -6.945e-02

Appendix C
River Valley Model With Plane At Base

max_disp50 = -9.050e-02
max_disp51 = -1.225e-01
max_disp52 = -1.700e-01
max_disp53 = -2.312e-01
max_disp54 = -2.952e-01
max_disp55 = -3.600e-01
max_disp56 = -4.214e-01
max_disp57 = -4.754e-01
max_disp58 = -5.190e-01
max_disp59 = -5.502e-01
max_disp60 = -2.362e+00
max_disp61 = -5.502e-01
max_disp62 = -5.190e-01
max_disp63 = -4.754e-01
max_disp64 = -4.214e-01
max_disp65 = -3.600e-01
max_disp66 = -2.952e-01
max_disp67 = -2.312e-01
max_disp68 = -1.700e-01
max_disp69 = -1.225e-01
max_disp70 = -9.050e-02
max_disp71 = -6.945e-02
max_disp72 = -5.516e-02
max_disp73 = -4.513e-02
max_disp74 = -3.810e-02
max_disp75 = -3.344e-02
max_disp76 = -3.024e-02
max_disp77 = -2.778e-02
max_disp78 = -2.563e-02
max_disp79 = -2.367e-02
max_disp80 = -2.185e-02
max_disp81 = -2.014e-02
max_disp82 = -1.854e-02
max_disp83 = -1.703e-02
max_disp84 = -1.562e-02
max_disp85 = -1.430e-02
max_disp86 = -1.306e-02
max_disp87 = -1.190e-02
max_disp88 = -1.081e-02
max_disp89 = -9.804e-03
max_disp90 = -8.861e-03

Appendix C
River Valley Model With Plane At Base

max_disp91 = -7.980e-03
max_disp92 = -7.159e-03
max_disp93 = -6.396e-03
max_disp94 = -5.686e-03
max_disp95 = -5.027e-03
max_disp96 = -4.413e-03
max_disp97 = -3.843e-03
max_disp98 = -3.313e-03
max_disp99 = -2.820e-03
max_disp100 = -2.362e-03
max_disp101 = -1.937e-03
max_disp102 = -1.542e-03
max_disp103 = -1.177e-03
max_disp104 = -8.401e-04
max_disp105 = -5.299e-04
max_disp106 = -2.455e-04
max_disp107 = 1.411e-05
max_disp108 = 2.494e-04
max_disp109 = 4.614e-04
max_disp110 = 6.505e-04
max_disp111 = 8.172e-04
max_disp112 = 9.621e-04
max_disp113 = 1.086e-03
max_disp114 = 1.188e-03
max_disp115 = 1.270e-03
max_disp116 = 1.331e-03
max_disp117 = 1.372e-03
max_disp118 = 1.394e-03
max_disp119 = 1.398e-03

*; Converting y-displacement into y-velocity via timestep and number of
cycles and assigning to corresponding gridpoints*

gp_yvel(gri_chk1) = max_disp1/(30000*tdel)
gp_yvel(gri_chk2) = max_disp2/(30000*tdel)
gp_yvel(gri_chk3) = max_disp3/(30000*tdel)
gp_yvel(gri_chk4) = max_disp4/(30000*tdel)
gp_yvel(gri_chk5) = max_disp5/(30000*tdel)
gp_yvel(gri_chk6) = max_disp6/(30000*tdel)
gp_yvel(gri_chk7) = max_disp7/(30000*tdel)
gp_yvel(gri_chk8) = max_disp8/(30000*tdel)

Appendix C
River Valley Model With Plane At Base

gp_yvel(gri_chk9) = max_disp9/(30000*tdel)
gp_yvel(gri_chk10) = max_disp10/(30000*tdel)
gp_yvel(gri_chk11) = max_disp11/(30000*tdel)
gp_yvel(gri_chk12) = max_disp12/(30000*tdel)
gp_yvel(gri_chk13) = max_disp13/(30000*tdel)
gp_yvel(gri_chk14) = max_disp14/(30000*tdel)
gp_yvel(gri_chk15) = max_disp15/(30000*tdel)
gp_yvel(gri_chk16) = max_disp16/(30000*tdel)
gp_yvel(gri_chk17) = max_disp17/(30000*tdel)
gp_yvel(gri_chk18) = max_disp18/(30000*tdel)
gp_yvel(gri_chk19) = max_disp19/(30000*tdel)
gp_yvel(gri_chk20) = max_disp20/(30000*tdel)
gp_yvel(gri_chk21) = max_disp21/(30000*tdel)
gp_yvel(gri_chk22) = max_disp22/(30000*tdel)
gp_yvel(gri_chk23) = max_disp23/(30000*tdel)
gp_yvel(gri_chk24) = max_disp24/(30000*tdel)
gp_yvel(gri_chk25) = max_disp25/(30000*tdel)
gp_yvel(gri_chk26) = max_disp26/(30000*tdel)
gp_yvel(gri_chk27) = max_disp27/(30000*tdel)
gp_yvel(gri_chk28) = max_disp28/(30000*tdel)
gp_yvel(gri_chk29) = max_disp29/(30000*tdel)
gp_yvel(gri_chk30) = max_disp30/(30000*tdel)
gp_yvel(gri_chk31) = max_disp31/(30000*tdel)
gp_yvel(gri_chk32) = max_disp32/(30000*tdel)
gp_yvel(gri_chk33) = max_disp33/(30000*tdel)
gp_yvel(gri_chk34) = max_disp34/(30000*tdel)
gp_yvel(gri_chk35) = max_disp35/(30000*tdel)
gp_yvel(gri_chk36) = max_disp36/(30000*tdel)
gp_yvel(gri_chk37) = max_disp37/(30000*tdel)
gp_yvel(gri_chk38) = max_disp38/(30000*tdel)
gp_yvel(gri_chk39) = max_disp39/(30000*tdel)
gp_yvel(gri_chk40) = max_disp40/(30000*tdel)
gp_yvel(gri_chk41) = max_disp41/(30000*tdel)
gp_yvel(gri_chk42) = max_disp42/(30000*tdel)
gp_yvel(gri_chk43) = max_disp43/(30000*tdel)
gp_yvel(gri_chk44) = max_disp44/(30000*tdel)
gp_yvel(gri_chk45) = max_disp45/(30000*tdel)
gp_yvel(gri_chk46) = max_disp46/(30000*tdel)
gp_yvel(gri_chk47) = max_disp47/(30000*tdel)
gp_yvel(gri_chk48) = max_disp48/(30000*tdel)
gp_yvel(gri_chk49) = max_disp49/(30000*tdel)

Appendix C
River Valley Model With Plane At Base

gp_yvel(gri_chk50) = max_disp50/(30000*tdel)
gp_yvel(gri_chk51) = max_disp51/(30000*tdel)
gp_yvel(gri_chk52) = max_disp52/(30000*tdel)
gp_yvel(gri_chk53) = max_disp53/(30000*tdel)
gp_yvel(gri_chk54) = max_disp54/(30000*tdel)
gp_yvel(gri_chk55) = max_disp55/(30000*tdel)
gp_yvel(gri_chk56) = max_disp56/(30000*tdel)
gp_yvel(gri_chk57) = max_disp57/(30000*tdel)
gp_yvel(gri_chk58) = max_disp58/(30000*tdel)
gp_yvel(gri_chk59) = max_disp59/(30000*tdel)
gp_yvel(gri_chk60) = max_disp60/(30000*tdel)
gp_yvel(gri_chk61) = max_disp61/(30000*tdel)
gp_yvel(gri_chk62) = max_disp62/(30000*tdel)
gp_yvel(gri_chk63) = max_disp63/(30000*tdel)
gp_yvel(gri_chk64) = max_disp64/(30000*tdel)
gp_yvel(gri_chk65) = max_disp65/(30000*tdel)
gp_yvel(gri_chk66) = max_disp66/(30000*tdel)
gp_yvel(gri_chk67) = max_disp67/(30000*tdel)
gp_yvel(gri_chk68) = max_disp68/(30000*tdel)
gp_yvel(gri_chk69) = max_disp69/(30000*tdel)
gp_yvel(gri_chk70) = max_disp70/(30000*tdel)
gp_yvel(gri_chk71) = max_disp71/(30000*tdel)
gp_yvel(gri_chk72) = max_disp72/(30000*tdel)
gp_yvel(gri_chk73) = max_disp73/(30000*tdel)
gp_yvel(gri_chk74) = max_disp74/(30000*tdel)
gp_yvel(gri_chk75) = max_disp75/(30000*tdel)
gp_yvel(gri_chk76) = max_disp76/(30000*tdel)
gp_yvel(gri_chk77) = max_disp77/(30000*tdel)
gp_yvel(gri_chk78) = max_disp78/(30000*tdel)
gp_yvel(gri_chk79) = max_disp79/(30000*tdel)
gp_yvel(gri_chk80) = max_disp80/(30000*tdel)
gp_yvel(gri_chk81) = max_disp81/(30000*tdel)
gp_yvel(gri_chk82) = max_disp82/(30000*tdel)
gp_yvel(gri_chk83) = max_disp83/(30000*tdel)
gp_yvel(gri_chk84) = max_disp84/(30000*tdel)
gp_yvel(gri_chk85) = max_disp85/(30000*tdel)
gp_yvel(gri_chk86) = max_disp86/(30000*tdel)
gp_yvel(gri_chk87) = max_disp87/(30000*tdel)
gp_yvel(gri_chk88) = max_disp88/(30000*tdel)
gp_yvel(gri_chk89) = max_disp89/(30000*tdel)
gp_yvel(gri_chk90) = max_disp90/(30000*tdel)

Appendix C
River Valley Model With Plane At Base

```
gp_yvel (gri_chk91) = max_disp91/(30000*tdel)
gp_yvel (gri_chk92) = max_disp92/(30000*tdel)
gp_yvel (gri_chk93) = max_disp93/(30000*tdel)
gp_yvel (gri_chk94) = max_disp94/(30000*tdel)
gp_yvel (gri_chk95) = max_disp95/(30000*tdel)
gp_yvel (gri_chk96) = max_disp96/(30000*tdel)
gp_yvel (gri_chk97) = max_disp97/(30000*tdel)
gp_yvel (gri_chk98) = max_disp98/(30000*tdel)
gp_yvel (gri_chk99) = max_disp99/(30000*tdel)
gp_yvel (gri_chk100) = max_disp100/(30000*tdel)
gp_yvel (gri_chk101) = max_disp101/(30000*tdel)
gp_yvel (gri_chk102) = max_disp102/(30000*tdel)
gp_yvel (gri_chk103) = max_disp103/(30000*tdel)
gp_yvel (gri_chk104) = max_disp104/(30000*tdel)
gp_yvel (gri_chk105) = max_disp105/(30000*tdel)
gp_yvel (gri_chk106) = max_disp106/(30000*tdel)
gp_yvel (gri_chk107) = max_disp107/(30000*tdel)
gp_yvel (gri_chk108) = max_disp108/(30000*tdel)
gp_yvel (gri_chk109) = max_disp109/(30000*tdel)
gp_yvel (gri_chk110) = max_disp110/(30000*tdel)
gp_yvel (gri_chk111) = max_disp111/(30000*tdel)
gp_yvel (gri_chk112) = max_disp112/(30000*tdel)
gp_yvel (gri_chk113) = max_disp113/(30000*tdel)
gp_yvel (gri_chk114) = max_disp114/(30000*tdel)
gp_yvel (gri_chk115) = max_disp115/(30000*tdel)
gp_yvel (gri_chk116) = max_disp116/(30000*tdel)
gp_yvel (gri_chk117) = max_disp117/(30000*tdel)
gp_yvel (gri_chk118) = max_disp118/(30000*tdel)
gp_yvel (gri_chk119) = max_disp119/(30000*tdel)
temp1 = gp_yvel (gri_chk1)
temp2 = gp_yvel (gri_chk2)
temp3 = gp_yvel (gri_chk3)
temp4 = gp_yvel (gri_chk4)
temp5 = gp_yvel (gri_chk5)
temp6 = gp_yvel (gri_chk6)
temp7 = gp_yvel (gri_chk7)
temp8 = gp_yvel (gri_chk8)
temp9 = gp_yvel (gri_chk9)
temp10 = gp_yvel (gri_chk10)
temp11 = gp_yvel (gri_chk11)
temp12 = gp_yvel (gri_chk12)
```

Appendix C
River Valley Model With Plane At Base

```
temp13 = gp_yvel (gri_chk13)
temp14 = gp_yvel (gri_chk14)
temp15 = gp_yvel (gri_chk15)
temp16 = gp_yvel (gri_chk16)
temp17 = gp_yvel (gri_chk17)
temp18 = gp_yvel (gri_chk18)
temp19 = gp_yvel (gri_chk19)
temp20 = gp_yvel (gri_chk20)
temp21 = gp_yvel (gri_chk21)
temp22 = gp_yvel (gri_chk22)
temp23 = gp_yvel (gri_chk23)
temp24 = gp_yvel (gri_chk24)
temp25 = gp_yvel (gri_chk25)
temp26 = gp_yvel (gri_chk26)
temp27 = gp_yvel (gri_chk27)
temp28 = gp_yvel (gri_chk28)
temp29 = gp_yvel (gri_chk29)
temp30 = gp_yvel (gri_chk30)
temp31 = gp_yvel (gri_chk31)
temp32 = gp_yvel (gri_chk32)
temp33 = gp_yvel (gri_chk33)
temp34 = gp_yvel (gri_chk34)
temp35 = gp_yvel (gri_chk35)
temp36 = gp_yvel (gri_chk36)
temp37 = gp_yvel (gri_chk37)
temp38 = gp_yvel (gri_chk38)
temp39 = gp_yvel (gri_chk39)
temp40 = gp_yvel (gri_chk40)
temp41 = gp_yvel (gri_chk41)
temp42 = gp_yvel (gri_chk42)
temp43 = gp_yvel (gri_chk43)
temp44 = gp_yvel (gri_chk44)
temp45 = gp_yvel (gri_chk45)
temp46 = gp_yvel (gri_chk46)
temp47 = gp_yvel (gri_chk47)
temp48 = gp_yvel (gri_chk48)
temp49 = gp_yvel (gri_chk49)
temp50 = gp_yvel (gri_chk50)
temp51 = gp_yvel (gri_chk51)
temp52 = gp_yvel (gri_chk52)
temp53 = gp_yvel (gri_chk53)
```


Appendix C
River Valley Model With Plane At Base

```
temp54 = gp_yvel (gri_chk54)
temp55 = gp_yvel (gri_chk55)
temp56 = gp_yvel (gri_chk56)
temp57 = gp_yvel (gri_chk57)
temp58 = gp_yvel (gri_chk58)
temp59 = gp_yvel (gri_chk59)
temp60 = gp_yvel (gri_chk60)
temp61 = gp_yvel (gri_chk61)
temp62 = gp_yvel (gri_chk62)
temp63 = gp_yvel (gri_chk63)
temp64 = gp_yvel (gri_chk64)
temp65 = gp_yvel (gri_chk65)
temp66 = gp_yvel (gri_chk66)
temp67 = gp_yvel (gri_chk67)
temp68 = gp_yvel (gri_chk68)
temp69 = gp_yvel (gri_chk69)
temp70 = gp_yvel (gri_chk70)
temp71 = gp_yvel (gri_chk71)
temp72 = gp_yvel (gri_chk72)
temp73 = gp_yvel (gri_chk73)
temp74 = gp_yvel (gri_chk74)
temp75 = gp_yvel (gri_chk75)
temp76 = gp_yvel (gri_chk76)
temp77 = gp_yvel (gri_chk77)
temp78 = gp_yvel (gri_chk78)
temp79 = gp_yvel (gri_chk79)
temp80 = gp_yvel (gri_chk80)
temp81 = gp_yvel (gri_chk81)
temp82 = gp_yvel (gri_chk82)
temp83 = gp_yvel (gri_chk83)
temp84 = gp_yvel (gri_chk84)
temp85 = gp_yvel (gri_chk85)
temp86 = gp_yvel (gri_chk86)
temp87 = gp_yvel (gri_chk87)
temp88 = gp_yvel (gri_chk88)
temp89 = gp_yvel (gri_chk89)
temp90 = gp_yvel (gri_chk90)
temp91 = gp_yvel (gri_chk91)
temp92 = gp_yvel (gri_chk92)
temp93 = gp_yvel (gri_chk93)
temp94 = gp_yvel (gri_chk94)
```

Appendix C
River Valley Model With Plane At Base

```
temp95 = gp_yvel(gri_chk95)
temp96 = gp_yvel(gri_chk96)
temp97 = gp_yvel(gri_chk97)
temp98 = gp_yvel(gri_chk98)
temp99 = gp_yvel(gri_chk99)
temp100 = gp_yvel(gri_chk100)
temp101 = gp_yvel(gri_chk101)
temp102 = gp_yvel(gri_chk102)
temp103 = gp_yvel(gri_chk103)
temp104 = gp_yvel(gri_chk104)
temp105 = gp_yvel(gri_chk105)
temp106 = gp_yvel(gri_chk106)
temp107 = gp_yvel(gri_chk107)
temp108 = gp_yvel(gri_chk108)
temp109 = gp_yvel(gri_chk109)
temp110 = gp_yvel(gri_chk110)
temp111 = gp_yvel(gri_chk111)
temp112 = gp_yvel(gri_chk112)
temp113 = gp_yvel(gri_chk113)
temp114 = gp_yvel(gri_chk114)
temp115 = gp_yvel(gri_chk115)
temp116 = gp_yvel(gri_chk116)
temp117 = gp_yvel(gri_chk117)
temp118 = gp_yvel(gri_chk118)
temp119 = gp_yvel(gri_chk119)
end
```

valleysolve

; Assigning y-velocities to base

```
bo yv temp1 ra -0.1 0.1 -189.1 -188.9
bo yv temp2 ra 4.4 4.6 -189.1 -188.9
bo yv temp3 ra 13.4 13.6 -189.1 -188.9
bo yv temp4 ra 22.4 22.6 -189.1 -188.9
bo yv temp5 ra 31.4 31.6 -189.1 -188.9
bo yv temp6 ra 40.4 40.6 -189.1 -188.9
bo yv temp7 ra 49.4 49.6 -189.1 -188.9
bo yv temp8 ra 58.4 58.6 -189.1 -188.9
bo yv temp9 ra 67.4 67.6 -189.1 -188.9
bo yv temp10 ra 76.4 76.6 -189.1 -188.9
```

Appendix C
River Valley Model With Plane At Base

bo yv temp11 ra 85.4 85.6 -189.1 -188.9
bo yv temp12 ra 94.4 94.6 -189.1 -188.9
bo yv temp13 ra 103.4 103.6 -189.1 -188.9
bo yv temp14 ra 112.4 112.6 -189.1 -188.9
bo yv temp15 ra 121.4 121.6 -189.1 -188.9
bo yv temp16 ra 130.4 130.6 -189.1 -188.9
bo yv temp17 ra 139.4 139.6 -189.1 -188.9
bo yv temp18 ra 148.4 148.6 -189.1 -188.9
bo yv temp19 ra 157.4 157.6 -189.1 -188.9
bo yv temp20 ra 166.4 166.6 -189.1 -188.9
bo yv temp21 ra 175.4 175.6 -189.1 -188.9
bo yv temp22 ra 184.4 184.6 -189.1 -188.9
bo yv temp23 ra 193.4 193.6 -189.1 -188.9
bo yv temp24 ra 202.4 202.6 -189.1 -188.9
bo yv temp25 ra 211.4 211.6 -189.1 -188.9
bo yv temp26 ra 220.4 220.6 -189.1 -188.9
bo yv temp27 ra 229.4 229.6 -189.1 -188.9
bo yv temp28 ra 238.4 238.6 -189.1 -188.9
bo yv temp29 ra 247.4 247.6 -189.1 -188.9
bo yv temp30 ra 256.4 256.6 -189.1 -188.9
bo yv temp31 ra 265.4 265.6 -189.1 -188.9
bo yv temp32 ra 274.4 274.6 -189.1 -188.9
bo yv temp33 ra 283.4 283.6 -189.1 -188.9
bo yv temp34 ra 292.4 292.6 -189.1 -188.9
bo yv temp35 ra 301.4 301.6 -189.1 -188.9
bo yv temp36 ra 310.4 310.6 -189.1 -188.9
bo yv temp37 ra 319.4 319.6 -189.1 -188.9
bo yv temp38 ra 328.4 328.6 -189.1 -188.9
bo yv temp39 ra 337.4 337.6 -189.1 -188.9
bo yv temp40 ra 346.4 346.6 -189.1 -188.9
bo yv temp41 ra 355.4 355.6 -189.1 -188.9
bo yv temp42 ra 364.4 364.6 -189.1 -188.9
bo yv temp43 ra 373.4 373.6 -189.1 -188.9
bo yv temp44 ra 382.4 382.6 -189.1 -188.9
bo yv temp45 ra 391.4 391.6 -189.1 -188.9
bo yv temp46 ra 400.4 400.6 -189.1 -188.9
bo yv temp47 ra 409.4 409.6 -189.1 -188.9
bo yv temp48 ra 418.4 418.6 -189.1 -188.9
bo yv temp49 ra 427.4 427.6 -189.1 -188.9
bo yv temp50 ra 436.4 436.6 -189.1 -188.9
bo yv temp51 ra 445.4 445.6 -189.1 -188.9

Appendix C
River Valley Model With Plane At Base

bo yv temp52 ra 454.4 454.6 -189.1 -188.9
bo yv temp53 ra 463.4 463.6 -189.1 -188.9
bo yv temp54 ra 472.4 472.6 -189.1 -188.9
bo yv temp55 ra 481.4 481.6 -189.1 -188.9
bo yv temp56 ra 490.4 490.6 -189.1 -188.9
bo yv temp57 ra 499.4 499.6 -189.1 -188.9
bo yv temp58 ra 508.4 508.6 -189.1 -188.9
bo yv temp59 ra 517.4 517.6 -189.1 -188.9
bo yv temp60 ra 524.9 525.1 -189.1 -188.9
bo yv temp61 ra 532.4 532.6 -189.1 -188.9
bo yv temp62 ra 541.4 541.6 -189.1 -188.9
bo yv temp63 ra 550.4 550.6 -189.1 -188.9
bo yv temp64 ra 559.4 559.6 -189.1 -188.9
bo yv temp65 ra 568.4 568.6 -189.1 -188.9
bo yv temp66 ra 577.4 577.6 -189.1 -188.9
bo yv temp67 ra 586.4 586.6 -189.1 -188.9
bo yv temp68 ra 595.4 595.6 -189.1 -188.9
bo yv temp69 ra 604.4 604.6 -189.1 -188.9
bo yv temp70 ra 613.4 613.6 -189.1 -188.9
bo yv temp71 ra 622.4 622.6 -189.1 -188.9
bo yv temp72 ra 631.4 631.6 -189.1 -188.9
bo yv temp73 ra 640.4 640.6 -189.1 -188.9
bo yv temp74 ra 649.4 649.6 -189.1 -188.9
bo yv temp75 ra 658.4 658.6 -189.1 -188.9
bo yv temp76 ra 667.4 667.6 -189.1 -188.9
bo yv temp77 ra 676.4 676.6 -189.1 -188.9
bo yv temp78 ra 685.4 685.6 -189.1 -188.9
bo yv temp79 ra 694.4 694.6 -189.1 -188.9
bo yv temp80 ra 703.4 703.6 -189.1 -188.9
bo yv temp81 ra 712.4 712.6 -189.1 -188.9
bo yv temp82 ra 721.4 721.6 -189.1 -188.9
bo yv temp83 ra 730.4 730.6 -189.1 -188.9
bo yv temp84 ra 739.4 739.6 -189.1 -188.9
bo yv temp85 ra 748.4 748.6 -189.1 -188.9
bo yv temp86 ra 757.4 757.6 -189.1 -188.9
bo yv temp87 ra 766.4 766.6 -189.1 -188.9
bo yv temp88 ra 775.4 775.6 -189.1 -188.9
bo yv temp89 ra 784.4 784.6 -189.1 -188.9
bo yv temp90 ra 793.4 793.6 -189.1 -188.9
bo yv temp91 ra 802.4 802.6 -189.1 -188.9
bo yv temp92 ra 811.4 811.6 -189.1 -188.9

Appendix C
River Valley Model With Plane At Base

bo yv temp93 ra 820.4 820.6 -189.1 -188.9
bo yv temp94 ra 829.4 829.6 -189.1 -188.9
bo yv temp95 ra 838.4 838.6 -189.1 -188.9
bo yv temp96 ra 847.4 847.6 -189.1 -188.9
bo yv temp97 ra 856.4 856.6 -189.1 -188.9
bo yv temp98 ra 865.4 865.6 -189.1 -188.9
bo yv temp99 ra 874.4 874.6 -189.1 -188.9
bo yv temp100 ra 883.4 883.6 -189.1 -188.9
bo yv temp101 ra 892.4 892.6 -189.1 -188.9
bo yv temp102 ra 901.4 901.6 -189.1 -188.9
bo yv temp103 ra 910.4 910.6 -189.1 -188.9
bo yv temp104 ra 919.4 919.6 -189.1 -188.9
bo yv temp105 ra 928.4 928.6 -189.1 -188.9
bo yv temp106 ra 937.4 937.6 -189.1 -188.9
bo yv temp107 ra 946.4 946.6 -189.1 -188.9
bo yv temp108 ra 955.4 955.6 -189.1 -188.9
bo yv temp109 ra 964.4 964.6 -189.1 -188.9
bo yv temp110 ra 973.4 973.6 -189.1 -188.9
bo yv temp111 ra 982.4 982.6 -189.1 -188.9
bo yv temp112 ra 991.4 991.6 -189.1 -188.9
bo yv temp113 ra 1000.4 1000.6 -189.1 -188.9
bo yv temp114 ra 1009.4 1009.6 -189.1 -188.9
bo yv temp115 ra 1018.4 1018.6 -189.1 -188.9
bo yv temp116 ra 1027.4 1027.6 -189.1 -188.9
bo yv temp117 ra 1036.4 1036.6 -189.1 -188.9
bo yv temp118 ra 1045.4 1045.6 -189.1 -188.9
bo yv temp119 ra 1049.9 1050.9 -189.1 -188.9

s 30000

; Resetting boundary conditions

bo yfr

bo xfr

bo yv 0 ra 0 1050 -200 -188.9

bo xv 0 ra -0.1 0.1 -189.1 0.1

bo xv 0 ra 1049.9 1050.1 -189.1 0.1

; Solving for final equilibrium

da a

so rat 1e-5 ste 1000000

sa valley1_ini2.sav

s 20000

sa valley1_final.sav

APPENDIX D

RIVER VALLEY MODEL WITH PLANE BELOW BASE

ti

Valley 1

; Creating model geometry

ro = 0.01

set ov = 0.2

bl 0,-189 0,0 1050,0 1050,-189

cr 0,-78 1050,-78 ; Hawkesbury Sandstone (78 m thick)

cr 0,-85 1050,-85 ; Newport Formation (7 m thick)

cr 0,-97 1050,-97 ; Bald Hill Claystone (9 m thick)

cr 0,-186 1050,-186 ; Bulgo Sandstone (89 m thick + 3 m thick beam)

; Generating vertical cracks for beam at base of Bald Hill Claystone

jr 0,-189 0,-186 525,-186 525,-189

js 90,0 3,0 0,0 9,0 13.5,-189

cr 525,-189 525,-186

cr 532.5,-189 532.5,-186

jr 532.5,-189 532.5,-186 1050,-186 1050,-189

js 90,0 3,0 0,0 9,0 1045.5,-189

; Generating pre-defined cracks for valleys (70 m deep x 50 m wide)

cr 0,-70 1050,-70

cr 0,-71 1050,-71 ; New translation plane 1 m below base of valley

cr 500,-70 500,0

cr 450,-70 450,0

cr 400,-70 400,0

cr 350,-70 350,0

cr 300,-70 300,0

cr 250,-70 250,0

Appendix D
River Valley Model With Plane Below Base

cr 200,-70 200,0
cr 150,-70 150,0
cr 100,-70 100,0
cr 50,-70 50,0
cr 550,-70 550,0
cr 600,-70 600,0
cr 650,-70 650,0
cr 700,-70 700,0
cr 750,-70 750,0
cr 800,-70 800,0
cr 850,-70 850,0
cr 900,-70 900,0
cr 950,-70 950,0
cr 1000,-70 1000,0

; Defining discontinuities

jr 0,-78 0,-71 1050,-71 1050,-78 ; Hawkesbury Sandstone
js 90,0 9,0 9,0 9,0 4.5 -78

jr 0,-85 0,-78 1050,-78 1050,-85 ; Newport Formation
js 0,0 1050,0 0,0 1,0
js 90,0 1,0 1,0 1,0
js 90,0 1,0 1,0 1,0 0.5,-79

jr 0,-97 0,-85 1050,-85 1050,-97 ; Bald Hill Claystone
js 0,0 1050,0 0,0 1,0
js 90,0 1,0 1,0 1,0
js 90,0 1,0 1,0 1,0 0.5,-87

jr 0,-186 0,-97 1050,-97 1050,-186 ; Bulgo Sandstone
js 0,0 525,0 0,0 9,0
js 90,0 9,0 9,0 9,0
js 90,0 9,0 9,0 9,0 4.5,-117
jr 0,-189 0,-186 525,-186 525,-189
js 90,0 3,0 0,0 9,0 13.5,-189
cr 525,-189 525,-186
cr 532.5,-189 532.5,-186
jr 532.5,-189 532.5,-186 1050,-186 1050,-189
js 90,0 3,0 0,0 9,0 1045.5,-189

Appendix D
River Valley Model With Plane Below Base

; Generating zones for deformable blocks

ge q 12.7 ra 0 1050 -70 0 ; Hawkesbury Sandstone
ge q 0.2 ra 0 1050 -71 -70 ; Beam
ge q 12.7 ra 0 1050 -78 -71 ; Hawkesbury Sandstone
ge q 1.4 ra 0 1050 -85 -78 ; Newport Formation
ge q 1.4 ra 0 1050 -97 -85 ; Bald Hill Claystone
ge q 12.7 ra 0 1050 -189 -97 ; Bulgo Sandstone

; Defining material properties

pro m 1 de = 2397 b = 11.47e9 sh = 5.65e9 coh = 9.70e6 fr= 37.25 &
ten = 3.58e6 ; Hawkesbury Sandstone

pro m 2 de = 2290 b = 7.77e9 sh = 4.66e9 coh = 8.85e6 fr= 35.00 &
ten = 3.40e6 ; Newport Formation

pro m 3 de = 2719 b = 14.12e9 sh = 4.72e9 coh = 10.60e6 fr= 27.80 &
ten = 2.90e6 ; Bald Hill Claystone

pro m 4 de = 2527 b = 12.60e9 sh = 7.91e9 coh = 17.72e6 fr= 35.40 &
ten = 6.55e6 ; Bulgo Sandstone

; Assigning material properties

ch cons 3

ch m 1 ra 0 1050 -78 0 ; Hawkesbury Sandstone
ch m 2 ra 0 1050 -85 -78 ; Newport Formation
ch m 3 ra 0 1050 -97 -85 ; Bald Hill Claystone
ch m 4 ra 0 1050 -189 -97 ; Bulgo Sandstone

; Defining bedding plane properties

pro jm = 1 jkn = 21e9 jks = 2.1e9 & ; Hawkesbury Sandstone
j f = 25 jrf = 15 &
j c = 0.29e6 jresc = 0

pro jm = 2 jkn = 140e9 jks = 14.0e9 & ; Newport Formation
j f = 25 jrf = 15 &
j c = 0.29e6 jresc = 0

Appendix D
River Valley Model With Plane Below Base

pro jm = 3 jkn = 204e9 jks = 20.4e9 & ; Bald Hill Claystone
j f = 25 jrf = 15 &
j c = 0.29e6 jresc = 0

pro jm = 4 jkn = 26e9 jks = 2.6e9 & ; Bulgo Sandstone
j f = 25 jrf = 15 &
j c = 0.29e6 jresc = 0

pro jm = 5 jkn = 204e9 jks = 20.4e9 & ; Beam
j f = 89 jrf = 89 &
j c = 1e10 jresc = 1e10 &
j t = 1e10 jrt = 1e10

; Assigning bedding plane properties

ch jc = 5 ra 0 1050 -189 0 ang -1 1
se jc = 5

ch jm 1 ra 0 1050 -78 0 ang -1 1 ; Hawkesbury Sandstone
ch jm 2 ra 0 1050 -85 -78 ang -1 1 ; Newport Formation
ch jm 3 ra 0 1050 -97 -85 ang -1 1 ; Bald Hill Claystone
ch jm 4 ra 0 1050 -186 -97 ang -1 1 ; Bulgo Sandstone
ch jm 5 ra 0 1050 -189 -186 ang -1 1 ; Beam

; Vertical joint properties

pro jm = 6 jkn = 21e9 jks = 2.1e9 & ; Hawkesbury Sandstone
j f = 19 jrf = 15 &
j c = 0.86e6 jresc = 0

pro jm = 7 jkn = 140e9 jks = 14.0e9 & ; Newport Formation
j f = 19 jrf = 15 &
j c = 0.86e6 jresc = 0

pro jm = 8 jkn = 204e9 jks = 20.4e9 & ; Bald Hill Claystone
j f = 19 jrf = 15 &
j c = 0.86e6 jresc = 0

pro jm = 9 jkn = 26e9 jks = 2.6e9 & ; Bulgo Sandstone;
j f = 19 jrf = 15 &
j c = 0.86e6 jresc = 0

Appendix D
River Valley Model With Plane Below Base

```
pro jm = 10 jkn = 204e9 jks = 20.4e9 & ; Beam
      jf = 89 jrf = 89 &
      jc = 1e10 jresc = 1e10 &
      jt = 1e10 jrt = 1e10

; Assigning vertical joint properties

ch jc = 5 ra 0 1050 -189 0 ang 89 91
se jc = 5

ch jm 6 ra 0 1050 -186 0 ang 89 91 ; Hawkesbury Sandstone
ch jm 7 ra 0 1050 -85 -78 ang 89 91 ; Newport Formation
ch jm 8 ra 0 1050 -97 -85 ang 89 91 ; Bald Hill Claystone
ch jm 9 ra 0 1050 -186 -97 ang 89 91 ; Bulgo Sandstone
ch jm 10 ra 0 1050 -189 -186 ang 89 91 ; Beam

; Defining gravity

se gr 0 -9.81

; Defining boundary conditions

bo yv 0 ra 0 1050 -189.1 -188.9
bo xv 0 ra -0.1 0.1 -189.1 0.1
bo xv 0 ra 1049.9 1050.1 -189.1 0.1

; Defining initial stress conditions

in st 0 0 0 yg 4.77e4 0 2.39e4 szz 0 zg 0 4.77e4 ra 0 1050 -189 0

sa valley1_ini1.sav

; Cycle to equilibrium

da a

so
```

Appendix D
River Valley Model With Plane Below Base

; Removing valley and cycle to equilibrium

de ra 500 550 -70 0

da a

so

; Removing boundary conditions at base and attaching pre-determined y-displacements

rese vel

rese di

bo yfr

bo xfr

bo xv 0 ra -0.1 0.1 -189.1 0.1

bo xv 0 ra 1049.9 1050.1 -189.1 0.1

; Histories

; X Displacements (valley closure)

; Top of valley

hi xd 50 0 ;1

hi xd 100 0 ;2

hi xd 150 0 ;3

hi xd 200 0 ;4

hi xd 250 0 ;5

hi xd 300 0 ;6

hi xd 350 0 ;7

hi xd 400 0 ;8

hi xd 450 0 ;9

hi xd 500 0 ;10

hi xd 550 0 ;11

; Y Displacements (subsidence)

hi yd 0 0 ;12

hi yd 25 0 ;13

hi yd 50 0 ;14

Appendix D
River Valley Model With Plane Below Base

hi yd 75 0 ;15
hi yd 100 0 ;16
hi yd 125 0 ;17
hi yd 150 0 ;18
hi yd 175 0 ;19
hi yd 200 0 ;20
hi yd 225 0 ;21
hi yd 250 0 ;22
hi yd 275 0 ;23
hi yd 300 0 ;24
hi yd 325 0 ;25
hi yd 350 0 ;26
hi yd 375 0 ;27
hi yd 400 0 ;28
hi yd 425 0 ;29
hi yd 450 0 ;30
hi yd 475 0 ;31
hi yd 500 0 ;32
hi yd 525 0 ;33
hi yd 550 0 ;34
hi yd 575 0 ;35
hi yd 600 0 ;36
hi yd 625 0 ;37
hi yd 650 0 ;38
hi yd 675 0 ;39
hi yd 700 0 ;40
hi yd 725 0 ;41
hi yd 750 0 ;42
hi yd 775 0 ;43
hi yd 800 0 ;44
hi yd 825 0 ;45
hi yd 850 0 ;46
hi yd 875 0 ;47
hi yd 900 0 ;48
hi yd 925 0 ;49
hi yd 950 0 ;50
hi yd 975 0 ;51
hi yd 1000 0 ;52
hi yd 1025 0 ;53
hi yd 1050 0 ;54

Appendix D
River Valley Model With Plane Below Base

; Y displacements (base)

hi yd 0 -189 ;55
hi yd 4.5 -189 ;56
hi yd 13.5 -189 ;57
hi yd 22.5 -189 ;58
hi yd 31.5 -189 ;59
hi yd 40.5 -189 ;60
hi yd 49.5 -189 ;61
hi yd 58.5 -189 ;62
hi yd 67.5 -189 ;63
hi yd 76.5 -189 ;64
hi yd 85.5 -189 ;65
hi yd 94.5 -189 ;66
hi yd 103.5 -189 ;67
hi yd 112.5 -189 ;68
hi yd 121.5 -189 ;69
hi yd 130.5 -189 ;70
hi yd 139.5 -189 ;71
hi yd 148.5 -189 ;72
hi yd 157.5 -189 ;73
hi yd 166.5 -189 ;74
hi yd 175.5 -189 ;75
hi yd 184.5 -189 ;76
hi yd 193.5 -189 ;77
hi yd 202.5 -189 ;78
hi yd 211.5 -189 ;79
hi yd 220.5 -189 ;80
hi yd 229.5 -189 ;81
hi yd 238.5 -189 ;82
hi yd 247.5 -189 ;83
hi yd 256.5 -189 ;84
hi yd 265.5 -189 ;85
hi yd 274.5 -189 ;86
hi yd 283.5 -189 ;87
hi yd 292.5 -189 ;88
hi yd 301.5 -189 ;89
hi yd 310.5 -189 ;90
hi yd 319.5 -189 ;91
hi yd 328.5 -189 ;92
hi yd 337.5 -189 ;93

Appendix D
River Valley Model With Plane Below Base

```
hi yd 346.5 -189 ;94
hi yd 355.5 -189 ;95
hi yd 364.5 -189 ;96
hi yd 373.5 -189 ;97
hi yd 382.5 -189 ;98
hi yd 391.5 -189 ;99
hi yd 400.5 -189 ;100
hi yd 409.5 -189 ;101
hi yd 418.5 -189 ;102
hi yd 427.5 -189 ;103
hi yd 436.5 -189 ;104
hi yd 445.5 -189 ;105
hi yd 454.5 -189 ;106
hi yd 463.5 -189 ;107
hi yd 472.5 -189 ;108
hi yd 481.5 -189 ;109
hi yd 490.5 -189 ;110
hi yd 499.5 -189 ;111
hi yd 508.5 -189 ;112
hi yd 517.5 -189 ;113
hi yd 525.0 -189 ;114
```

; Creating y-velocities at base and final solving routine

```
def valleysolve
```

; Step 1 to obtain time step

```
command
```

```
cyc 1
```

```
end_command
```

; Identifying gridpoints at base to which velocities will be attached

```
gri_chk1 = gp_near(0.0, -189)
gri_chk2 = gp_near(4.5, -189)
gri_chk3 = gp_near(13.5, -189)
gri_chk4 = gp_near(22.5, -189)
gri_chk5 = gp_near(31.5, -189)
gri_chk6 = gp_near(40.5, -189)
gri_chk7 = gp_near(49.5, -189)
```

Appendix D
River Valley Model With Plane Below Base

gri_chk8 = gp_near(58.5, -189)
gri_chk9 = gp_near(67.5, -189)
gri_chk10 = gp_near(76.5, -189)
gri_chk11 = gp_near(85.5, -189)
gri_chk12 = gp_near(94.5, -189)
gri_chk13 = gp_near(103.5, -189)
gri_chk14 = gp_near(112.5, -189)
gri_chk15 = gp_near(121.5, -189)
gri_chk16 = gp_near(130.5, -189)
gri_chk17 = gp_near(139.5, -189)
gri_chk18 = gp_near(148.5, -189)
gri_chk19 = gp_near(157.5, -189)
gri_chk20 = gp_near(166.5, -189)
gri_chk21 = gp_near(175.5, -189)
gri_chk22 = gp_near(184.5, -189)
gri_chk23 = gp_near(193.5, -189)
gri_chk24 = gp_near(202.5, -189)
gri_chk25 = gp_near(211.5, -189)
gri_chk26 = gp_near(220.5, -189)
gri_chk27 = gp_near(229.5, -189)
gri_chk28 = gp_near(238.5, -189)
gri_chk29 = gp_near(247.5, -189)
gri_chk30 = gp_near(256.5, -189)
gri_chk31 = gp_near(265.5, -189)
gri_chk32 = gp_near(274.5, -189)
gri_chk33 = gp_near(283.5, -189)
gri_chk34 = gp_near(292.5, -189)
gri_chk35 = gp_near(301.5, -189)
gri_chk36 = gp_near(310.5, -189)
gri_chk37 = gp_near(319.5, -189)
gri_chk38 = gp_near(328.5, -189)
gri_chk39 = gp_near(337.5, -189)
gri_chk40 = gp_near(346.5, -189)
gri_chk41 = gp_near(355.5, -189)
gri_chk42 = gp_near(364.5, -189)
gri_chk43 = gp_near(373.5, -189)
gri_chk44 = gp_near(382.5, -189)
gri_chk45 = gp_near(391.5, -189)
gri_chk46 = gp_near(400.5, -189)
gri_chk47 = gp_near(409.5, -189)
gri_chk48 = gp_near(418.5, -189)

Appendix D
River Valley Model With Plane Below Base

gri_chk49 = gp_near(427.5, -189)
gri_chk50 = gp_near(436.5, -189)
gri_chk51 = gp_near(445.5, -189)
gri_chk52 = gp_near(454.5, -189)
gri_chk53 = gp_near(463.5, -189)
gri_chk54 = gp_near(472.5, -189)
gri_chk55 = gp_near(481.5, -189)
gri_chk56 = gp_near(490.5, -189)
gri_chk57 = gp_near(499.5, -189)
gri_chk58 = gp_near(508.5, -189)
gri_chk59 = gp_near(517.5, -189)
gri_chk60 = gp_near(525.0, -189)
gri_chk61 = gp_near(532.5, -189)
gri_chk62 = gp_near(541.5, -189)
gri_chk63 = gp_near(550.5, -189)
gri_chk64 = gp_near(559.5, -189)
gri_chk65 = gp_near(568.5, -189)
gri_chk66 = gp_near(577.5, -189)
gri_chk67 = gp_near(586.5, -189)
gri_chk68 = gp_near(595.5, -189)
gri_chk69 = gp_near(604.5, -189)
gri_chk70 = gp_near(613.5, -189)
gri_chk71 = gp_near(622.5, -189)
gri_chk72 = gp_near(631.5, -189)
gri_chk73 = gp_near(640.5, -189)
gri_chk74 = gp_near(649.5, -189)
gri_chk75 = gp_near(658.5, -189)
gri_chk76 = gp_near(667.5, -189)
gri_chk77 = gp_near(676.5, -189)
gri_chk78 = gp_near(685.5, -189)
gri_chk79 = gp_near(694.5, -189)
gri_chk80 = gp_near(703.5, -189)
gri_chk81 = gp_near(712.5, -189)
gri_chk82 = gp_near(721.5, -189)
gri_chk83 = gp_near(730.5, -189)
gri_chk84 = gp_near(739.5, -189)
gri_chk85 = gp_near(748.5, -189)
gri_chk86 = gp_near(757.5, -189)
gri_chk87 = gp_near(766.5, -189)
gri_chk88 = gp_near(775.5, -189)
gri_chk89 = gp_near(784.5, -189)

Appendix D
River Valley Model With Plane Below Base

```
gri_chk90 = gp_near(793.5, -189)
gri_chk91 = gp_near(802.5, -189)
gri_chk92 = gp_near(811.5, -189)
gri_chk93 = gp_near(820.5, -189)
gri_chk94 = gp_near(829.5, -189)
gri_chk95 = gp_near(838.5, -189)
gri_chk96 = gp_near(847.5, -189)
gri_chk97 = gp_near(856.5, -189)
gri_chk98 = gp_near(865.5, -189)
gri_chk99 = gp_near(874.5, -189)
gri_chk100 = gp_near(883.5, -189)
gri_chk101 = gp_near(892.5, -189)
gri_chk102 = gp_near(901.5, -189)
gri_chk103 = gp_near(910.5, -189)
gri_chk104 = gp_near(919.5, -189)
gri_chk105 = gp_near(928.5, -189)
gri_chk106 = gp_near(937.5, -189)
gri_chk107 = gp_near(946.5, -189)
gri_chk108 = gp_near(955.5, -189)
gri_chk109 = gp_near(964.5, -189)
gri_chk110 = gp_near(973.5, -189)
gri_chk111 = gp_near(982.5, -189)
gri_chk112 = gp_near(991.5, -189)
gri_chk113 = gp_near(1000.5, -189)
gri_chk114 = gp_near(1009.5, -189)
gri_chk115 = gp_near(1018.5, -189)
gri_chk116 = gp_near(1027.5, -189)
gri_chk117 = gp_near(1036.5, -189)
gri_chk118 = gp_near(1045.5, -189)
gri_chk119 = gp_near(1050.0, -189)
```

; Defining y-displacements from Model 4

```
max_disp1 = 1.398e-03
max_disp2 = 1.394e-03
max_disp3 = 1.372e-03
max_disp4 = 1.331e-03
max_disp5 = 1.270e-03
max_disp6 = 1.188e-03
max_disp7 = 1.086e-03
max_disp8 = 9.621e-04
```

Appendix D
River Valley Model With Plane Below Base

max_disp9 = 8.172e-04
max_disp10 = 6.505e-04
max_disp11 = 4.614e-04
max_disp12 = 2.494e-04
max_disp13 = 1.411e-05
max_disp14 = -2.455e-04
max_disp15 = -5.299e-04
max_disp16 = -8.401e-04
max_disp17 = -1.177e-03
max_disp18 = -1.542e-03
max_disp19 = -1.937e-03
max_disp20 = -2.362e-03
max_disp21 = -2.820e-03
max_disp22 = -3.313e-03
max_disp23 = -3.843e-03
max_disp24 = -4.413e-03
max_disp25 = -5.027e-03
max_disp26 = -5.686e-03
max_disp27 = -6.396e-03
max_disp28 = -7.159e-03
max_disp29 = -7.980e-03
max_disp30 = -8.861e-03
max_disp31 = -9.804e-03
max_disp32 = -1.081e-02
max_disp33 = -1.190e-02
max_disp34 = -1.306e-02
max_disp35 = -1.430e-02
max_disp36 = -1.562e-02
max_disp37 = -1.703e-02
max_disp38 = -1.854e-02
max_disp39 = -2.014e-02
max_disp40 = -2.185e-02
max_disp41 = -2.367e-02
max_disp42 = -2.563e-02
max_disp43 = -2.778e-02
max_disp44 = -3.024e-02
max_disp45 = -3.344e-02
max_disp46 = -3.810e-02
max_disp47 = -4.513e-02
max_disp48 = -5.516e-02
max_disp49 = -6.945e-02

Appendix D
River Valley Model With Plane Below Base

max_disp50 = -9.050e-02
max_disp51 = -1.225e-01
max_disp52 = -1.700e-01
max_disp53 = -2.312e-01
max_disp54 = -2.952e-01
max_disp55 = -3.600e-01
max_disp56 = -4.214e-01
max_disp57 = -4.754e-01
max_disp58 = -5.190e-01
max_disp59 = -5.502e-01
max_disp60 = -2.362e+00
max_disp61 = -5.502e-01
max_disp62 = -5.190e-01
max_disp63 = -4.754e-01
max_disp64 = -4.214e-01
max_disp65 = -3.600e-01
max_disp66 = -2.952e-01
max_disp67 = -2.312e-01
max_disp68 = -1.700e-01
max_disp69 = -1.225e-01
max_disp70 = -9.050e-02
max_disp71 = -6.945e-02
max_disp72 = -5.516e-02
max_disp73 = -4.513e-02
max_disp74 = -3.810e-02
max_disp75 = -3.344e-02
max_disp76 = -3.024e-02
max_disp77 = -2.778e-02
max_disp78 = -2.563e-02
max_disp79 = -2.367e-02
max_disp80 = -2.185e-02
max_disp81 = -2.014e-02
max_disp82 = -1.854e-02
max_disp83 = -1.703e-02
max_disp84 = -1.562e-02
max_disp85 = -1.430e-02
max_disp86 = -1.306e-02
max_disp87 = -1.190e-02
max_disp88 = -1.081e-02
max_disp89 = -9.804e-03
max_disp90 = -8.861e-03

Appendix D
River Valley Model With Plane Below Base

max_disp91 = -7.980e-03
max_disp92 = -7.159e-03
max_disp93 = -6.396e-03
max_disp94 = -5.686e-03
max_disp95 = -5.027e-03
max_disp96 = -4.413e-03
max_disp97 = -3.843e-03
max_disp98 = -3.313e-03
max_disp99 = -2.820e-03
max_disp100 = -2.362e-03
max_disp101 = -1.937e-03
max_disp102 = -1.542e-03
max_disp103 = -1.177e-03
max_disp104 = -8.401e-04
max_disp105 = -5.299e-04
max_disp106 = -2.455e-04
max_disp107 = 1.411e-05
max_disp108 = 2.494e-04
max_disp109 = 4.614e-04
max_disp110 = 6.505e-04
max_disp111 = 8.172e-04
max_disp112 = 9.621e-04
max_disp113 = 1.086e-03
max_disp114 = 1.188e-03
max_disp115 = 1.270e-03
max_disp116 = 1.331e-03
max_disp117 = 1.372e-03
max_disp118 = 1.394e-03
max_disp119 = 1.398e-03

*; Converting y-displacement into y-velocity via timestep and number of
cycles and assigning to corresponding gridpoints*

gp_yvel(gri_chk1) = max_disp1/(30000*tdel)
gp_yvel(gri_chk2) = max_disp2/(30000*tdel)
gp_yvel(gri_chk3) = max_disp3/(30000*tdel)
gp_yvel(gri_chk4) = max_disp4/(30000*tdel)
gp_yvel(gri_chk5) = max_disp5/(30000*tdel)
gp_yvel(gri_chk6) = max_disp6/(30000*tdel)
gp_yvel(gri_chk7) = max_disp7/(30000*tdel)
gp_yvel(gri_chk8) = max_disp8/(30000*tdel)

Appendix D
River Valley Model With Plane Below Base

gp_yvel(gri_chk9) = max_disp9/(30000*tdel)
gp_yvel(gri_chk10) = max_disp10/(30000*tdel)
gp_yvel(gri_chk11) = max_disp11/(30000*tdel)
gp_yvel(gri_chk12) = max_disp12/(30000*tdel)
gp_yvel(gri_chk13) = max_disp13/(30000*tdel)
gp_yvel(gri_chk14) = max_disp14/(30000*tdel)
gp_yvel(gri_chk15) = max_disp15/(30000*tdel)
gp_yvel(gri_chk16) = max_disp16/(30000*tdel)
gp_yvel(gri_chk17) = max_disp17/(30000*tdel)
gp_yvel(gri_chk18) = max_disp18/(30000*tdel)
gp_yvel(gri_chk19) = max_disp19/(30000*tdel)
gp_yvel(gri_chk20) = max_disp20/(30000*tdel)
gp_yvel(gri_chk21) = max_disp21/(30000*tdel)
gp_yvel(gri_chk22) = max_disp22/(30000*tdel)
gp_yvel(gri_chk23) = max_disp23/(30000*tdel)
gp_yvel(gri_chk24) = max_disp24/(30000*tdel)
gp_yvel(gri_chk25) = max_disp25/(30000*tdel)
gp_yvel(gri_chk26) = max_disp26/(30000*tdel)
gp_yvel(gri_chk27) = max_disp27/(30000*tdel)
gp_yvel(gri_chk28) = max_disp28/(30000*tdel)
gp_yvel(gri_chk29) = max_disp29/(30000*tdel)
gp_yvel(gri_chk30) = max_disp30/(30000*tdel)
gp_yvel(gri_chk31) = max_disp31/(30000*tdel)
gp_yvel(gri_chk32) = max_disp32/(30000*tdel)
gp_yvel(gri_chk33) = max_disp33/(30000*tdel)
gp_yvel(gri_chk34) = max_disp34/(30000*tdel)
gp_yvel(gri_chk35) = max_disp35/(30000*tdel)
gp_yvel(gri_chk36) = max_disp36/(30000*tdel)
gp_yvel(gri_chk37) = max_disp37/(30000*tdel)
gp_yvel(gri_chk38) = max_disp38/(30000*tdel)
gp_yvel(gri_chk39) = max_disp39/(30000*tdel)
gp_yvel(gri_chk40) = max_disp40/(30000*tdel)
gp_yvel(gri_chk41) = max_disp41/(30000*tdel)
gp_yvel(gri_chk42) = max_disp42/(30000*tdel)
gp_yvel(gri_chk43) = max_disp43/(30000*tdel)
gp_yvel(gri_chk44) = max_disp44/(30000*tdel)
gp_yvel(gri_chk45) = max_disp45/(30000*tdel)
gp_yvel(gri_chk46) = max_disp46/(30000*tdel)
gp_yvel(gri_chk47) = max_disp47/(30000*tdel)
gp_yvel(gri_chk48) = max_disp48/(30000*tdel)
gp_yvel(gri_chk49) = max_disp49/(30000*tdel)

Appendix D
River Valley Model With Plane Below Base

gp_yvel(gri_chk50) = max_disp50/(30000*tdel)
gp_yvel(gri_chk51) = max_disp51/(30000*tdel)
gp_yvel(gri_chk52) = max_disp52/(30000*tdel)
gp_yvel(gri_chk53) = max_disp53/(30000*tdel)
gp_yvel(gri_chk54) = max_disp54/(30000*tdel)
gp_yvel(gri_chk55) = max_disp55/(30000*tdel)
gp_yvel(gri_chk56) = max_disp56/(30000*tdel)
gp_yvel(gri_chk57) = max_disp57/(30000*tdel)
gp_yvel(gri_chk58) = max_disp58/(30000*tdel)
gp_yvel(gri_chk59) = max_disp59/(30000*tdel)
gp_yvel(gri_chk60) = max_disp60/(30000*tdel)
gp_yvel(gri_chk61) = max_disp61/(30000*tdel)
gp_yvel(gri_chk62) = max_disp62/(30000*tdel)
gp_yvel(gri_chk63) = max_disp63/(30000*tdel)
gp_yvel(gri_chk64) = max_disp64/(30000*tdel)
gp_yvel(gri_chk65) = max_disp65/(30000*tdel)
gp_yvel(gri_chk66) = max_disp66/(30000*tdel)
gp_yvel(gri_chk67) = max_disp67/(30000*tdel)
gp_yvel(gri_chk68) = max_disp68/(30000*tdel)
gp_yvel(gri_chk69) = max_disp69/(30000*tdel)
gp_yvel(gri_chk70) = max_disp70/(30000*tdel)
gp_yvel(gri_chk71) = max_disp71/(30000*tdel)
gp_yvel(gri_chk72) = max_disp72/(30000*tdel)
gp_yvel(gri_chk73) = max_disp73/(30000*tdel)
gp_yvel(gri_chk74) = max_disp74/(30000*tdel)
gp_yvel(gri_chk75) = max_disp75/(30000*tdel)
gp_yvel(gri_chk76) = max_disp76/(30000*tdel)
gp_yvel(gri_chk77) = max_disp77/(30000*tdel)
gp_yvel(gri_chk78) = max_disp78/(30000*tdel)
gp_yvel(gri_chk79) = max_disp79/(30000*tdel)
gp_yvel(gri_chk80) = max_disp80/(30000*tdel)
gp_yvel(gri_chk81) = max_disp81/(30000*tdel)
gp_yvel(gri_chk82) = max_disp82/(30000*tdel)
gp_yvel(gri_chk83) = max_disp83/(30000*tdel)
gp_yvel(gri_chk84) = max_disp84/(30000*tdel)
gp_yvel(gri_chk85) = max_disp85/(30000*tdel)
gp_yvel(gri_chk86) = max_disp86/(30000*tdel)
gp_yvel(gri_chk87) = max_disp87/(30000*tdel)
gp_yvel(gri_chk88) = max_disp88/(30000*tdel)
gp_yvel(gri_chk89) = max_disp89/(30000*tdel)
gp_yvel(gri_chk90) = max_disp90/(30000*tdel)

Appendix D
River Valley Model With Plane Below Base

```
gp_yvel(gri_chk91) = max_disp91/(30000*tdel)
gp_yvel(gri_chk92) = max_disp92/(30000*tdel)
gp_yvel(gri_chk93) = max_disp93/(30000*tdel)
gp_yvel(gri_chk94) = max_disp94/(30000*tdel)
gp_yvel(gri_chk95) = max_disp95/(30000*tdel)
gp_yvel(gri_chk96) = max_disp96/(30000*tdel)
gp_yvel(gri_chk97) = max_disp97/(30000*tdel)
gp_yvel(gri_chk98) = max_disp98/(30000*tdel)
gp_yvel(gri_chk99) = max_disp99/(30000*tdel)
gp_yvel(gri_chk100) = max_disp100/(30000*tdel)
gp_yvel(gri_chk101) = max_disp101/(30000*tdel)
gp_yvel(gri_chk102) = max_disp102/(30000*tdel)
gp_yvel(gri_chk103) = max_disp103/(30000*tdel)
gp_yvel(gri_chk104) = max_disp104/(30000*tdel)
gp_yvel(gri_chk105) = max_disp105/(30000*tdel)
gp_yvel(gri_chk106) = max_disp106/(30000*tdel)
gp_yvel(gri_chk107) = max_disp107/(30000*tdel)
gp_yvel(gri_chk108) = max_disp108/(30000*tdel)
gp_yvel(gri_chk109) = max_disp109/(30000*tdel)
gp_yvel(gri_chk110) = max_disp110/(30000*tdel)
gp_yvel(gri_chk111) = max_disp111/(30000*tdel)
gp_yvel(gri_chk112) = max_disp112/(30000*tdel)
gp_yvel(gri_chk113) = max_disp113/(30000*tdel)
gp_yvel(gri_chk114) = max_disp114/(30000*tdel)
gp_yvel(gri_chk115) = max_disp115/(30000*tdel)
gp_yvel(gri_chk116) = max_disp116/(30000*tdel)
gp_yvel(gri_chk117) = max_disp117/(30000*tdel)
gp_yvel(gri_chk118) = max_disp118/(30000*tdel)
gp_yvel(gri_chk119) = max_disp119/(30000*tdel)
temp1 = gp_yvel(gri_chk1)
temp2 = gp_yvel(gri_chk2)
temp3 = gp_yvel(gri_chk3)
temp4 = gp_yvel(gri_chk4)
temp5 = gp_yvel(gri_chk5)
temp6 = gp_yvel(gri_chk6)
temp7 = gp_yvel(gri_chk7)
temp8 = gp_yvel(gri_chk8)
temp9 = gp_yvel(gri_chk9)
temp10 = gp_yvel(gri_chk10)
temp11 = gp_yvel(gri_chk11)
temp12 = gp_yvel(gri_chk12)
```


Appendix D
River Valley Model With Plane Below Base

```
temp13 = gp_yvel (gri_chk13)
temp14 = gp_yvel (gri_chk14)
temp15 = gp_yvel (gri_chk15)
temp16 = gp_yvel (gri_chk16)
temp17 = gp_yvel (gri_chk17)
temp18 = gp_yvel (gri_chk18)
temp19 = gp_yvel (gri_chk19)
temp20 = gp_yvel (gri_chk20)
temp21 = gp_yvel (gri_chk21)
temp22 = gp_yvel (gri_chk22)
temp23 = gp_yvel (gri_chk23)
temp24 = gp_yvel (gri_chk24)
temp25 = gp_yvel (gri_chk25)
temp26 = gp_yvel (gri_chk26)
temp27 = gp_yvel (gri_chk27)
temp28 = gp_yvel (gri_chk28)
temp29 = gp_yvel (gri_chk29)
temp30 = gp_yvel (gri_chk30)
temp31 = gp_yvel (gri_chk31)
temp32 = gp_yvel (gri_chk32)
temp33 = gp_yvel (gri_chk33)
temp34 = gp_yvel (gri_chk34)
temp35 = gp_yvel (gri_chk35)
temp36 = gp_yvel (gri_chk36)
temp37 = gp_yvel (gri_chk37)
temp38 = gp_yvel (gri_chk38)
temp39 = gp_yvel (gri_chk39)
temp40 = gp_yvel (gri_chk40)
temp41 = gp_yvel (gri_chk41)
temp42 = gp_yvel (gri_chk42)
temp43 = gp_yvel (gri_chk43)
temp44 = gp_yvel (gri_chk44)
temp45 = gp_yvel (gri_chk45)
temp46 = gp_yvel (gri_chk46)
temp47 = gp_yvel (gri_chk47)
temp48 = gp_yvel (gri_chk48)
temp49 = gp_yvel (gri_chk49)
temp50 = gp_yvel (gri_chk50)
temp51 = gp_yvel (gri_chk51)
temp52 = gp_yvel (gri_chk52)
temp53 = gp_yvel (gri_chk53)
```

Appendix D
River Valley Model With Plane Below Base

```
temp54 = gp_yvel (gri_chk54)
temp55 = gp_yvel (gri_chk55)
temp56 = gp_yvel (gri_chk56)
temp57 = gp_yvel (gri_chk57)
temp58 = gp_yvel (gri_chk58)
temp59 = gp_yvel (gri_chk59)
temp60 = gp_yvel (gri_chk60)
temp61 = gp_yvel (gri_chk61)
temp62 = gp_yvel (gri_chk62)
temp63 = gp_yvel (gri_chk63)
temp64 = gp_yvel (gri_chk64)
temp65 = gp_yvel (gri_chk65)
temp66 = gp_yvel (gri_chk66)
temp67 = gp_yvel (gri_chk67)
temp68 = gp_yvel (gri_chk68)
temp69 = gp_yvel (gri_chk69)
temp70 = gp_yvel (gri_chk70)
temp71 = gp_yvel (gri_chk71)
temp72 = gp_yvel (gri_chk72)
temp73 = gp_yvel (gri_chk73)
temp74 = gp_yvel (gri_chk74)
temp75 = gp_yvel (gri_chk75)
temp76 = gp_yvel (gri_chk76)
temp77 = gp_yvel (gri_chk77)
temp78 = gp_yvel (gri_chk78)
temp79 = gp_yvel (gri_chk79)
temp80 = gp_yvel (gri_chk80)
temp81 = gp_yvel (gri_chk81)
temp82 = gp_yvel (gri_chk82)
temp83 = gp_yvel (gri_chk83)
temp84 = gp_yvel (gri_chk84)
temp85 = gp_yvel (gri_chk85)
temp86 = gp_yvel (gri_chk86)
temp87 = gp_yvel (gri_chk87)
temp88 = gp_yvel (gri_chk88)
temp89 = gp_yvel (gri_chk89)
temp90 = gp_yvel (gri_chk90)
temp91 = gp_yvel (gri_chk91)
temp92 = gp_yvel (gri_chk92)
temp93 = gp_yvel (gri_chk93)
temp94 = gp_yvel (gri_chk94)
```

Appendix D
River Valley Model With Plane Below Base

```
temp95 = gp_yvel(gri_chk95)
temp96 = gp_yvel(gri_chk96)
temp97 = gp_yvel(gri_chk97)
temp98 = gp_yvel(gri_chk98)
temp99 = gp_yvel(gri_chk99)
temp100 = gp_yvel(gri_chk100)
temp101 = gp_yvel(gri_chk101)
temp102 = gp_yvel(gri_chk102)
temp103 = gp_yvel(gri_chk103)
temp104 = gp_yvel(gri_chk104)
temp105 = gp_yvel(gri_chk105)
temp106 = gp_yvel(gri_chk106)
temp107 = gp_yvel(gri_chk107)
temp108 = gp_yvel(gri_chk108)
temp109 = gp_yvel(gri_chk109)
temp110 = gp_yvel(gri_chk110)
temp111 = gp_yvel(gri_chk111)
temp112 = gp_yvel(gri_chk112)
temp113 = gp_yvel(gri_chk113)
temp114 = gp_yvel(gri_chk114)
temp115 = gp_yvel(gri_chk115)
temp116 = gp_yvel(gri_chk116)
temp117 = gp_yvel(gri_chk117)
temp118 = gp_yvel(gri_chk118)
temp119 = gp_yvel(gri_chk119)
end
```

valleysolve

; Assigning y-velocities to base

```
bo yv temp1 ra -0.1 0.1 -189.1 -188.9
bo yv temp2 ra 4.4 4.6 -189.1 -188.9
bo yv temp3 ra 13.4 13.6 -189.1 -188.9
bo yv temp4 ra 22.4 22.6 -189.1 -188.9
bo yv temp5 ra 31.4 31.6 -189.1 -188.9
bo yv temp6 ra 40.4 40.6 -189.1 -188.9
bo yv temp7 ra 49.4 49.6 -189.1 -188.9
bo yv temp8 ra 58.4 58.6 -189.1 -188.9
bo yv temp9 ra 67.4 67.6 -189.1 -188.9
bo yv temp10 ra 76.4 76.6 -189.1 -188.9
```

Appendix D
River Valley Model With Plane Below Base

bo yv temp11 ra	85.4	85.6	-189.1	-188.9
bo yv temp12 ra	94.4	94.6	-189.1	-188.9
bo yv temp13 ra	103.4	103.6	-189.1	-188.9
bo yv temp14 ra	112.4	112.6	-189.1	-188.9
bo yv temp15 ra	121.4	121.6	-189.1	-188.9
bo yv temp16 ra	130.4	130.6	-189.1	-188.9
bo yv temp17 ra	139.4	139.6	-189.1	-188.9
bo yv temp18 ra	148.4	148.6	-189.1	-188.9
bo yv temp19 ra	157.4	157.6	-189.1	-188.9
bo yv temp20 ra	166.4	166.6	-189.1	-188.9
bo yv temp21 ra	175.4	175.6	-189.1	-188.9
bo yv temp22 ra	184.4	184.6	-189.1	-188.9
bo yv temp23 ra	193.4	193.6	-189.1	-188.9
bo yv temp24 ra	202.4	202.6	-189.1	-188.9
bo yv temp25 ra	211.4	211.6	-189.1	-188.9
bo yv temp26 ra	220.4	220.6	-189.1	-188.9
bo yv temp27 ra	229.4	229.6	-189.1	-188.9
bo yv temp28 ra	238.4	238.6	-189.1	-188.9
bo yv temp29 ra	247.4	247.6	-189.1	-188.9
bo yv temp30 ra	256.4	256.6	-189.1	-188.9
bo yv temp31 ra	265.4	265.6	-189.1	-188.9
bo yv temp32 ra	274.4	274.6	-189.1	-188.9
bo yv temp33 ra	283.4	283.6	-189.1	-188.9
bo yv temp34 ra	292.4	292.6	-189.1	-188.9
bo yv temp35 ra	301.4	301.6	-189.1	-188.9
bo yv temp36 ra	310.4	310.6	-189.1	-188.9
bo yv temp37 ra	319.4	319.6	-189.1	-188.9
bo yv temp38 ra	328.4	328.6	-189.1	-188.9
bo yv temp39 ra	337.4	337.6	-189.1	-188.9
bo yv temp40 ra	346.4	346.6	-189.1	-188.9
bo yv temp41 ra	355.4	355.6	-189.1	-188.9
bo yv temp42 ra	364.4	364.6	-189.1	-188.9
bo yv temp43 ra	373.4	373.6	-189.1	-188.9
bo yv temp44 ra	382.4	382.6	-189.1	-188.9
bo yv temp45 ra	391.4	391.6	-189.1	-188.9
bo yv temp46 ra	400.4	400.6	-189.1	-188.9
bo yv temp47 ra	409.4	409.6	-189.1	-188.9
bo yv temp48 ra	418.4	418.6	-189.1	-188.9
bo yv temp49 ra	427.4	427.6	-189.1	-188.9
bo yv temp50 ra	436.4	436.6	-189.1	-188.9
bo yv temp51 ra	445.4	445.6	-189.1	-188.9

Appendix D
River Valley Model With Plane Below Base

bo yv temp52 ra 454.4 454.6 -189.1 -188.9
bo yv temp53 ra 463.4 463.6 -189.1 -188.9
bo yv temp54 ra 472.4 472.6 -189.1 -188.9
bo yv temp55 ra 481.4 481.6 -189.1 -188.9
bo yv temp56 ra 490.4 490.6 -189.1 -188.9
bo yv temp57 ra 499.4 499.6 -189.1 -188.9
bo yv temp58 ra 508.4 508.6 -189.1 -188.9
bo yv temp59 ra 517.4 517.6 -189.1 -188.9
bo yv temp60 ra 524.9 525.1 -189.1 -188.9
bo yv temp61 ra 532.4 532.6 -189.1 -188.9
bo yv temp62 ra 541.4 541.6 -189.1 -188.9
bo yv temp63 ra 550.4 550.6 -189.1 -188.9
bo yv temp64 ra 559.4 559.6 -189.1 -188.9
bo yv temp65 ra 568.4 568.6 -189.1 -188.9
bo yv temp66 ra 577.4 577.6 -189.1 -188.9
bo yv temp67 ra 586.4 586.6 -189.1 -188.9
bo yv temp68 ra 595.4 595.6 -189.1 -188.9
bo yv temp69 ra 604.4 604.6 -189.1 -188.9
bo yv temp70 ra 613.4 613.6 -189.1 -188.9
bo yv temp71 ra 622.4 622.6 -189.1 -188.9
bo yv temp72 ra 631.4 631.6 -189.1 -188.9
bo yv temp73 ra 640.4 640.6 -189.1 -188.9
bo yv temp74 ra 649.4 649.6 -189.1 -188.9
bo yv temp75 ra 658.4 658.6 -189.1 -188.9
bo yv temp76 ra 667.4 667.6 -189.1 -188.9
bo yv temp77 ra 676.4 676.6 -189.1 -188.9
bo yv temp78 ra 685.4 685.6 -189.1 -188.9
bo yv temp79 ra 694.4 694.6 -189.1 -188.9
bo yv temp80 ra 703.4 703.6 -189.1 -188.9
bo yv temp81 ra 712.4 712.6 -189.1 -188.9
bo yv temp82 ra 721.4 721.6 -189.1 -188.9
bo yv temp83 ra 730.4 730.6 -189.1 -188.9
bo yv temp84 ra 739.4 739.6 -189.1 -188.9
bo yv temp85 ra 748.4 748.6 -189.1 -188.9
bo yv temp86 ra 757.4 757.6 -189.1 -188.9
bo yv temp87 ra 766.4 766.6 -189.1 -188.9
bo yv temp88 ra 775.4 775.6 -189.1 -188.9
bo yv temp89 ra 784.4 784.6 -189.1 -188.9
bo yv temp90 ra 793.4 793.6 -189.1 -188.9
bo yv temp91 ra 802.4 802.6 -189.1 -188.9
bo yv temp92 ra 811.4 811.6 -189.1 -188.9

Appendix D
River Valley Model With Plane Below Base

```
bo yv temp93 ra 820.4 820.6 -189.1 -188.9
bo yv temp94 ra 829.4 829.6 -189.1 -188.9
bo yv temp95 ra 838.4 838.6 -189.1 -188.9
bo yv temp96 ra 847.4 847.6 -189.1 -188.9
bo yv temp97 ra 856.4 856.6 -189.1 -188.9
bo yv temp98 ra 865.4 865.6 -189.1 -188.9
bo yv temp99 ra 874.4 874.6 -189.1 -188.9
bo yv temp100 ra 883.4 883.6 -189.1 -188.9
bo yv temp101 ra 892.4 892.6 -189.1 -188.9
bo yv temp102 ra 901.4 901.6 -189.1 -188.9
bo yv temp103 ra 910.4 910.6 -189.1 -188.9
bo yv temp104 ra 919.4 919.6 -189.1 -188.9
bo yv temp105 ra 928.4 928.6 -189.1 -188.9
bo yv temp106 ra 937.4 937.6 -189.1 -188.9
bo yv temp107 ra 946.4 946.6 -189.1 -188.9
bo yv temp108 ra 955.4 955.6 -189.1 -188.9
bo yv temp109 ra 964.4 964.6 -189.1 -188.9
bo yv temp110 ra 973.4 973.6 -189.1 -188.9
bo yv temp111 ra 982.4 982.6 -189.1 -188.9
bo yv temp112 ra 991.4 991.6 -189.1 -188.9
bo yv temp113 ra 1000.4 1000.6 -189.1 -188.9
bo yv temp114 ra 1009.4 1009.6 -189.1 -188.9
bo yv temp115 ra 1018.4 1018.6 -189.1 -188.9
bo yv temp116 ra 1027.4 1027.6 -189.1 -188.9
bo yv temp117 ra 1036.4 1036.6 -189.1 -188.9
bo yv temp118 ra 1045.4 1045.6 -189.1 -188.9
bo yv temp119 ra 1049.9 1050.9 -189.1 -188.9
```

s 30000

; Resetting boundary conditions

bo yfr

bo xfr

bo yv 0 ra 0 1050 -200 -188.9

bo xv 0 ra -0.1 0.1 -189.1 0.1

bo xv 0 ra 1049.9 1050.1 -189.1 0.1

; Solving for final equilibrium

da a

so rat 1e-5 ste 1000000

sa valley1_ini2.sav

s 20000

sa valley1_final.sav

APPENDIX E

VOUSSOIR BEAM THEORY

E.1 INTRODUCTION

It has been shown in the past that voussoir beam theory can be applied to mining subsidence problems quite effectively (Seedsman 2004), provided that there is a massive spanning unit in the overburden that remains elastic, the material properties of the spanning unit and overburden are known, and the characteristics of the cave zone is known.

Instead of providing a complete analysis and derivation of all the expressions required to calculate deflection with the voussoir beam theory, only the idealised three-joint voussoir beam model will be shown and the formulas required to determine beam deflection will be presented. The formulas presented are easily incorporated into a spreadsheet to make quick assessments of beams and the results from the analysis for Models 1 to 4 will be presented. The complete derivation can be found in Sofianos (1996) and Sofianos and Kapenis (1998), and further advancement on the topic as applied to multi-jointed beams can be found in Nomikos, Sofianos and Tsoutrelis (2002).

E.2 VOUSSOIR BEAM THEORY

Figure E.1 illustrates a three-joint voussoir beam model.

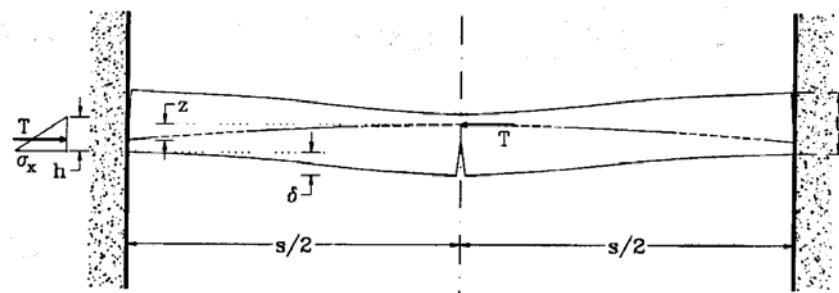


Fig. E.1 – Three-joint symmetric voussoir rock beam (Sofianos & Kapenis 1998)

The following assumptions are made:

- Rock is homogeneous, isotropic and elastic,
- The beam is horizontal and symmetric, is uniformly loaded and has only three vertical joints, one at the midspan and one at each end of the abutments,
- The abutment supports are rigid and the joints are very stiff,
- The rock Poisson's ratio is zero, and
- There is no lateral stress confining the beam prior to its deflection.

The calculation process is performed by following Equations E.1 to E.8.

$$Q_n = k_q \frac{S\gamma}{E} \quad [\text{E.1}]$$

$$S_n = \frac{S}{t} \quad [\text{E.2}]$$

$$n = 0.3 - 0.14s_n \sqrt[3]{Q_n} \quad [\text{E.3}]$$

$$z_{0n} = 1 - \frac{2}{3}n \quad [\text{E.4}]$$

$$s_z = \frac{S_n}{z_{0n}} \quad [\text{E.5}]$$

$$\delta_z = \frac{Q_n S_z^3}{16} \quad [\text{E.6}]$$

$$z_0 = z_{0n} t \quad [\text{E.7}]$$

$$\delta = \delta_z z_0 \quad [\text{E.8}]$$

Where,

- Q = Total weight of the voussoir beam
- k_q = Ratio of total load on the voussoir beam to its self weight
- S = Clear span of the voussoir beam
- γ = Unit weight of the rock comprising the voussoir beam
- E = Young's modulus of the rock comprising the voussoir beam
- n = Normalised contact length at the abutment or midspan
- z = Lever arm of the horizontal thrust couple
- δ = Vertical deflection of the rock beam at midspan

The subscripts (unless otherwise stated) are as follows:

- n = Normalisation of s or Q by division with t or tE , respectively
- 0 = Corresponding to the undeformed geometry of the beam
- z = Normalisation of lengths by division with z_0

Once the beam deflection has been calculated, the factor of safety against buckling (FS_b) can be assessed with Equation E.9.

$$FS_b = \frac{3.15}{Q_n s_z^3} \quad [E.9]$$

Finally, for a certain span of the beam the limiting thickness which corresponds to a factor of safety equal to one may be assessed from Equation E.10.

$$t_{\min} \approx \frac{s}{z_{0n}} \sqrt[3]{\frac{Q_n}{3.15}} \quad [E.10]$$

It is important to note that these analytical solutions have been verified numerically with UDEC (Sofianos 1996; and Sofianos & Kapenis 1998).

In the Bulgo Sandstone analysis, the predicted deflection is quite sensitive to the chosen value of n and the goaf angle (which is used in calculating the resulting surcharge).

Using an n value of 0.75 has proven to be effective whilst it has also been stated that for a large number of joints, n is between 0.18 and 0.30 (Nomikos, Sofianos & Tsoutrelis 2002). The values of n used in the Bulgo Sandstone analysis have been calculated using Equation E.3.